

CHARACTERIZING KNH: A MULTIFUNCTIONAL *KINGELLA KINGAE* ADHESIN

Bradley K. Kern

A DISSERTATION

in

Cell and Molecular Biology

Presented to the Faculties of the University of Pennsylvania

in

Partial Fulfillment of the Requirements for the

Degree of Doctor of Philosophy

2018

Supervisor of Dissertation

Joseph St. Geme, III, M.D., Chair, Department of Pediatrics

Graduate Group Chairperson

Daniel S. Kessler, Ph.D., Chair, Cell and Molecular Biology Graduate Group

Dissertation Committee

Mecky Pohlschroder, Ph.D., Professor of Biology

Igor Brodsky, Ph.D., Assistant Professor of Microbiology

Sunny Shin, Ph.D., Assistant Professor of Microbiology

Dustin Brisson, Ph.D., Associate Professor of Biology

CHARACTERIZING KNH: A MULTIFUNCTIONAL KINGELLA KINGAE ADHESIN

© 2018

Bradley K. Kern

Dedication

This work is dedicated to my wife Sarah, who has been my rock and inspiration through all of this.

Acknowledgements

I would like to thank my advisor Dr. Joseph St. Geme for giving me the opportunity to complete my graduate work in his lab. His advice and guidance have helped me to develop as a researcher. He has given me the independence and opportunity to learn new techniques and bring them to the lab to study bacterial adherence and for that I am grateful.

I would like to thank Dr. Eric Porsch for being a mentor and friend. His work on *Kingella kingae* was important in laying the groundwork for my project. In his role as lab den mother, he has put up with the incessant questions from my fellow labmates and myself with patience and aplomb. I would like to thank the other members of the St. Geme lab, past and present. From challenging questions during lab meetings, to obsessing over onesies, they have made lab life fun and entertaining. Thank you.

I would like to thank my committee members Dr. Mecky Pohlschroder, Dr. Dustin Brisson, Dr. Igor Brodsky, and Dr. Sunny Shin. Their guidance and enthusiasm for my work has always been insightful and encouraging.

Many thanks go to Dr. Pablo Yagupsky, Soroka University Medical Center, Ben-Gurion University of the Negev, Israel, for providing to us the collection of clinical isolates studied in this work.

For their assistance with chapter 2, I would like to thank Ray Meade and Biao Zuo from the University of Pennsylvania Electron Microscopy Resource Laboratory for assistance with the TEM work and Dr. Matthew Brukman from the University of Pennsylvania Nano-Bio Interface Center's Probe Facility for assistance with the AFM work.

For help with the sequencing project in chapter 3, I would like to thank Dr. Johnathan Schug and the University of Pennsylvania Next Generation Sequencing Core who performed the Illumina sequencing. Dr. Paul Planet of the Children's Hospital of Philadelphia and Apurva Narechania of the American Museum of Natural History in New York City assisted with genome assembly and analysis. Thank you.

ABSTRACT

CHARACTERIZING KNH: A MULTIFUNCTIONAL *KINGELLA KINGAE* ADHESIN

Bradley K. Kern

Joseph St. Geme, III, M.D.

Kingella kingae is an important pathogen in young children and initiates infection by colonizing the posterior pharynx. Adherence to pharyngeal epithelial cells is an important first step in the process of colonization. In the work presented here we examine the characteristics of the *Kingella kingae* trimeric autotransporter adhesin Knh.

Initially, we sought to elucidate the interplay of Knh with type IV pili (T4P) and the polysaccharide capsule in *K. kingae* adherence to epithelial cells. A strain expressing only Knh is capable of higher levels of adherence under shear stress than a strain expressing only T4P. Examination by various microscopy methods revealed that the capsule has a mean depth of 700 nm and that Knh is approximately 110 nm long. Additional microscopy demonstrated that when bacteria expressing retractile T4P are in close contact with host cells, the capsule is absent at the point of contact between the bacterium and the host cell membrane. Capsule depth remains intact, and adherence levels are markedly reduced with a retraction deficient mutant. These results support

the following model: T4P make initial contact with the host cell and mediate low strength adherence. T4P retract, pulling the organism closer to the host cell and displacing the capsule, allowing Knh to be exposed and mediate high strength, tight adherence to the host cell surface. This report provides the first description of the mechanical displacement of capsule enabling intimate bacterial adherence to host cells.

Further study of Knh revealed that Knh varies clonally among clinical isolates and contain regions of significant identity and regions of significant variation. Knh variants from clinical isolates are able to mediate adherence to epithelial cells and several extracellular matrix (ECM) proteins. However, the Knh variants vary in the specific ECM proteins to which they adhere. Using the Knh variant from our prototype strain, we observed that both the head and stalk domains of Knh can mediate adherence to epithelial cells and vitronectin. Knh is thus a multifunctional adhesin that is potentially important for colonization and the pathogenesis of *K. kingae* disease.

TABLE OF CONTENTS

DEDICATION.....	III
ACKNOWLEDGEMENTS.....	IV
ABSTRACT	VI
TABLE OF CONTENTS	VIII
LIST OF TABLES.....	X
LIST OF FIGURES	XI
CHAPTER 1. INTRODUCTION	1
1.1 History and general epidemiology	1
1.2 Polysaccharide capsules	5
1.3 Type IV pili	10
1.4 Trimeric autotransporter adhesins	12
1.5 Models of shear stress and bacterial adherence.....	19
1.6 Model of <i>K. kingae</i> adherence to host cells	20
1.7 Dissertation overview	22
CHAPTER 2: DEFINING THE MECHANICAL DETERMINANTS OF <i>KINGELLA KINGAE</i> ADHERENCE TO HOST CELLS	23
2.1 Introduction	23
2.2 Results	25
2.3 Discussion	33
2.4 Materials and Methods	37

CHAPTER 3: KNH IS A MULTIFUNCTIONAL ADHESIN PRODUCED BY <i>KINGELLA KINGAE</i>	46
3.1 Introduction	46
3.2 Results	48
3.3 Discussion	57
3.4 Materials and Methods	62
CHAPTER 4 SUMMARY AND FUTURE DIRECTIONS	71
4.1 Summary	71
4.2 Define the host receptor(s) of Knh	71
4.3 Determine the relationship of Knh structure, flexibility and adhesive activity	73
4.4 Define the extent of Knh variation among clinical isolates	76
4.5 Determine the role of Knh in pathogenesis	77
4.6 Determine whether Knh is antigenic	78
4.7 Knh and virulence gene regulation	80
BIBLIOGRAPHY	84

LIST OF TABLES

Chapter 2:

Table 1. Strain list	43
----------------------	----

Chapter 3:

Table 1. Strain list	69
----------------------	----

Table 2. Overlap PCR primers	70
------------------------------	----

LIST OF FIGURES

Chapter 1:

Figure 1. TEM micrographs of cationic ferritin stained capsule	9
Figure 2. EM micrograph of Knh on the surface of <i>K. kingae</i>	15
Figure 3. Model of <i>K. kingae</i> adherence to host cells	22

Chapter 2:

Figure 1. Shear resistance adherence assays	26
Figure 2. Inoculating under shear adherence assays	28
Figure 3. Depth of <i>K. kingae</i> capsule versus Knh length	30
Figure 4. Capsule displacement and T4P retraction	32
Figure S1. Representative frames from SRA assays	44
Figure S2. Western blot of <i>K. kingae</i> outer membrane preparations	45

Chapter 3:

Figure 1. Knh variability among clinical isolates	49
Figure 2. Knh variant adherence to host cells	52
Figure 3. YLHD and stalk region adherence to Chang cells	53
Figure 4. Knh variant adherence to ECM proteins	55
Figure 5. Knh YLHD and stalk region adhering to rhVN	56

Chapter 1. Introduction

1.1 History and general epidemiology

1.1.1 History

Kingella kingae is a pediatric pathobiont and a member of the Neisseriaceae family of gram-negative bacteria. *K. kingae* was first isolated by CDC microbiologist Elizabeth King in the 1960's and was originally classified as a *Moraxella* species. King unfortunately passed away before her findings could be published, and follow up work by Henriksen and Bovre established that this organism was in fact a novel species which they named *M. kingii* in honor of King (Henriksen and Bovre 1968). Later investigation demonstrated that the organism is substantially different from other *Moraxella* species, and thus it was placed in its own genus *Kingella* (Henriksen 1976).

1.1.2 Early epidemiology and emergence

K. kingae is difficult to culture under standard conditions and was therefore considered a rare cause of disease for the first several decades of its history (Yagupsky and Dagan 1997, Yagupsky 2004). Improved culture methods developed in the 1990's using blood culture vials increased the recognition of *K. kingae* as a cause of pediatric infections (Yagupsky, Dagan et al. 1992).

Recent developments in molecular diagnostic methods using PCR have revealed that a significant proportion of *K. kingae* infections likely go undiagnosed. The implementation of PCR detection methods has revealed that 50-80% of invasive disease cases in children 6-36 months of age are missed by culture detection alone (Verdier, Gayet-Ageron et al. 2005, Chometon, Benito et al. 2007). Using PCR for diagnosis, *K. kingae* accounts for ~80% of septic arthritis cases in children age 6-48 months.

Recently, PCR-based detection methods have also been used to study asymptomatic oropharyngeal carriage among children in Switzerland and New Zealand (Anderson de la Llana, Dubois-Ferriere et al. 2015, Olijve, Podmore et al. 2016) revealing carriage rates of 8.7% and 22.9%, respectively. These rates are in line with studies in Israel, which report carriage rates in young children around 10%. In comparison, a recent study in Australia of carriage using only culture methods was unable to detect any *K. kingae* carriage in a cohort of children in the susceptible age range (Khatami, Rivers et al. 2017).

One common target of PCR based screening strategies has been the RTX toxin gene (Ceroni, Cherkaoui et al. 2010, Lehours, Freydiere et al. 2011). Interestingly, a recent report revealed that the closely related species *K. negevensis* has an *rtxA* gene that is indistinguishable from the *K. kingae* *rtxA* gene (El Houmami, Bzdrenga et al. 2017). Subsequently, *groEL* has been reported to be a more specific candidate target for PCR

diagnosis (El Houmami, Fournier et al. 2017). Regardless, PCR-based screening has become an important tool for diagnosing *K. kingae* infection.

1.1.3 Epidemiology of colonization and disease

Epidemiological studies have demonstrated that *K. kingae* colonizes children between the ages of 6 and 48 months. Between 40% and 70% of children will be colonized at some point during the period of 6-48 months of age, with daycare attendance being a significant risk factor for colonization (Yagupsky, Dagan et al. 1995, Amit, Dagan et al. 2013, Amit, Flaishmakher et al. 2014). Longitudinal studies have demonstrated a carriage rate of 10% on average, though a study in New Zealand observed a carriage rate as high as 22.9% (Olijve, Podmore et al. 2016). Colonization can last weeks to months and is often intermittent or recurrent (Yagupsky, Dagan et al. 1995, Slonim, Walker et al. 1998, Amit, Flaishmakher et al. 2014). In a daycare setting, a single strain or clonal group often predominates within the facility, sometimes with strain replacement over time (Slonim, Walker et al. 1998). Strains colonizing a daycare facility are often unique to a particular facility when compared to neighboring facilities (Sena, Seed et al. 2010, Bidet, Collin et al. 2013). Adults are not typically colonized by *K. kingae*, unless they frequently come into contact with colonized children, such as daycare workers (Brandle, Spyropoulou et al. 2016).

Outbreaks of *K. kingae* invasive disease are also often associated with daycare facilities (Yagupsky 2014). Observed attack rates of exposed individuals have been reported to

be approximately 14% to 25% (Kiang, Ogunmodede et al. 2005, Yagupsky, Erlich et al. 2006, Bidet, Collin et al. 2013, Yagupsky, Ben-Ami et al. 2016). Asymptomatic carriage rates in facilities experiencing an outbreak tend to be higher than the average, with rates as high as ~70%.

Colonization of the oropharynx is positively associated with *K. kingae* invasive disease (Gravel, Ceroni et al. 2017). Studies of paired isolates from the oropharynx and blood or synovial exudate of children presenting with *K. kingae* invasive disease suggest that invasive disease proceeds from colonization of the posterior pharynx (Yagupsky, Porat et al. 2009, Basmaci, Ilharreborde et al. 2012). After colonization, *K. kingae* can breach the pharyngeal epithelium, enter the bloodstream, and disseminate to sites of disease. Breaching of the pharyngeal epithelium is thought to be facilitated by viral coinfection (Anderson de la Llana, Dubois-Ferriere et al. 2015, Basmaci, Bonacorsi et al. 2015, Droz, Enouf et al. 2018) and/or the potent *K. kingae* RTX (Kehl-Fie and St Geme 2007, Chang, Nudell et al. 2014). *K. kingae* causes osteomyelitis, occult bacteremia, and more rarely endocarditis, in addition to septic arthritis. Susceptibility to *K. kingae* invasive disease correlates with waning maternal antibody titers against *K. kingae* and decreases with the development of the child's own adaptive immunity (Slonim, Steiner et al. 2003, Spyropoulou, Brandle et al. 2017).

K. kingae strains are widely variable in their ability to cause disease. Several clonal groups/sequence types are significantly associated with invasive disease (Amit, Porat et

al. 2012). Five clonal groups identified by pulse field gel electrophoresis (PFGE), B, H, K, N, and P, comprise 72% of all invasive disease cases in one study. Clonal group K is associated with occult bacteremia, clonal group N with septic arthritis and osteomyelitis, and clonal group P with endocarditis. Other clonal groups are almost never found in cases of invasive disease and are associated with asymptomatic carriage.

Adherence to respiratory epithelium is an important first step in colonization. Previous work in our lab identified three factors that interact to either mediate or modulate adherence to host cells: a polysaccharide capsule, type IV pili (T4P), and the trimeric autotransporter adhesin (TAA) Knh (Porsch, Kehl-Fie et al. 2012).

1.2 Polysaccharide capsules

1.2.1 Biology of capsules

Capsules are composed of polysaccharide chains anchored by a lipid moiety to the bacterial outer membrane. Capsules are best recognized as a virulence factor contributing to serum resistance by preventing opsonization of the organism through the masking of surface antigens in a variety of gram-negative and gram-positive bacteria (Hallstrom and Riesbeck 2010, Hill, Griffiths et al. 2010, Miajlovic and Smith 2014). It has also been observed that capsules can inhibit biofilm formation and autoaggregation and sterically inhibit adherence to surfaces and host cells (Misawa, Kelley et al. 2015, Tu, Hsieh et al. 2015).

Capsular polysaccharides are highly hydrated and organized. The coordination of water molecules and ions can cause polymers to become networked or interwoven. This networking confers the properties of a gel-like coating around the bacterium. The insertion of other bacterial surface factors such as fimbriae into and throughout the capsule can further change the surface properties of the capsule (Wang, Wilksch et al. 2015) in a way measurable by atomic force microscopy (AFM).

1.2.2 Imaging capsules

Imaging capsules for studies of their structure in relationship to bacteria can be challenging. Negative and positive stains of capsules and imaging by light microscopy have been used to detect capsules on the surface of a variety of bacteria (Richardson and Sadoff 1977, Babb and Cummins 1978, Reimann, Heise et al. 1988). However, these methods rely on the ability of the capsule to exclude or take up the stain and for the microscopy to be of high enough resolution to detect the area of exclusion or staining corresponding to capsule. Higher resolution microscopy methods such as TEM combined with stains that have enhanced contrast have increased our ability to reliably image capsules.

K. kingae encapsulation has been confirmed via TEM in our lab (Porsch, Kehl-Fie et al. 2012, Starr, Porsch et al. 2016). Many capsules can be visualized by TEM using a cationic ferritin stain. Samples are fixed and stained with the cationic stain, which is capable of permeating and adhering to the negatively charged capsular polysaccharides.

When viewed by TEM, the stained layer of capsule appears as an electron dense halo surrounding the bacterium (Figure 1). This method is useful for viewing the presence and continuity of capsule around a bacterium.

A weakness of cationic ferritin staining and similar methods is that they can result in the collapse of capsule due to the dehydrating effects of fixation during sample preparation. This dehydration makes measurements of capsule depth difficult to interpret using these methods (Stukalov, Korenevsky et al. 2008). Recently, AFM has been used to measure hydrated capsule, as AFM can be done in an aqueous environment (Wang, Wilksch et al. 2015, Mularski, Wilksch et al. 2016). The gel-like property of capsules gives them resistance to deformation by the AFM probe tip. The depth of capsule - as well as other traits such as turgor - can be determined by analysis of the deformation resistance force curves.

The mechanical properties of capsules as measured by AFM can be modeled using four mathematical models that correspond to different phases of capsule deformation (Wang, Wilksch et al. 2015). The first phase is modeled by long range double layer interactions; this gives the distance at which ionic repulsion or attraction between the capsule and the probe tip occurs and is called the Debye length. The second phase represents the deformation of the capsule polysaccharides and is fit by the Pincus theory for compression of a polyelectrolyte brush. This number is dependent on the length of the polysaccharides and their density on the cell surface. The third phase occurs when the

fully compressed polysaccharide chains are further compacted and is fit by the Hertz model. The fourth phase is initiated when the cell membrane begins to directly support the force of indentation and is fit by Hooke's law.

A simplified model was introduced by Mularski et al. (2016) and defined the capsule depth as the distance between the onset of the AFM probe tip deflection and the onset of the linear force regime fit by Hooke's law, which indicates indentation of the cellular membrane. This simplified model assumes the Debye length given by the double layer interactions is negligible in deionized water or low salt buffer. AFM is therefore an accurate method for measuring and imaging bacterial capsules under hydrating conditions.

1.2.3 Capsule of *K. kingae*

All *K. kingae* isolates examined to date contain one to three capsule synthesis genes, the *lipA* and *lipB* genes encoding β Kdo transferases, and an ABC-type capsule export system encoded by the *ctrABCD* genes (Starr, Porsch et al. 2016). The synthesis genes, the export genes, *lipA*, and *lipB* are located in physically separate regions of the *K. kingae* chromosome, different from the arrangement in most encapsulated bacteria. Disruption of any of these loci results in a nonencapsulated strain. Disruption of the *ctrABCD* capsule transport locus does not prevent the production of capsular polysaccharides, and these polysaccharides accumulate within lacunae visible by

transmission electron microscopy (TEM) and are detectable by chemical assays in whole cell sonicates.

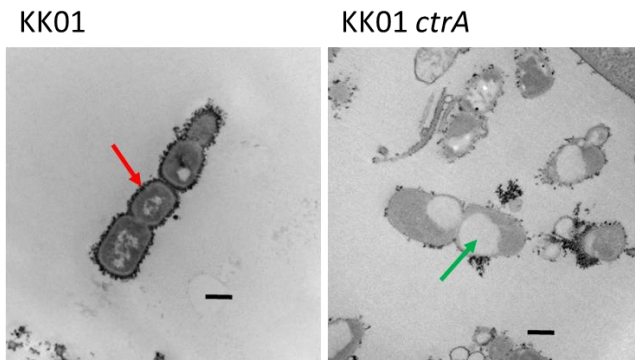


Figure 1. TEM micrographs of a) wild type KK01 demonstrating the electron dense halo of cationic ferritin staining (red arrow) and b) KK01 *ctrA* mutant strain with capsule filled lacunae (green arrow). Scale bar is 500 nm.

Work in our lab has determined that *K. kinage* expresses four distinct capsule type, each characterized by unique combinations of constituent saccharides and linkages (Starr, Porsch et al. 2016). Each capsule type is encoded by a distinct capsule synthesis gene locus. Epidemiological analysis of the distribution of the capsule types has revealed that the types a and b capsules are overrepresented among clinical isolates from sites of invasive disease as compared to isolates from asymptomatic carriers (Starr, Porsch et al. 2016, Porsch, Starr et al. 2017).

1.3 Type IV pili

1.3.1 Biosynthesis and composition

T4P are long, flexible surface fibers produced by bacteria. T4P are important adhesive structures expressed by bacteria and have been shown to be important factors in various functions such as motility, biofilm formation, autoaggregation, and natural competence in gram-negative bacteria (Berry and Pelicic 2015, Maier and Wong 2015, Chang 2017). Each fiber is composed of polymerized pilin subunits that associate via a hydrophobic tail (Leighton, Buensuceso et al. 2015, Hospenthal, Costa et al. 2017). In *K. kingae*, the major pilin subunit is PilA1 (Kehl-Fie, Miller et al. 2008). Additional minor pilins and other pilus-associated proteins are incorporated into the pilus and it has been suggested that these confer functionality to the pilus (Leong, Bloomfield et al. 2017). The core pilus secretion complex is composed of a periplasm-spanning scaffold, outer membrane pore, and extension/retraction machinery, all of which function to secrete and anchor the pilus to the cell surface (Hospenthal, Costa et al. 2017).

T4P biosynthesis in *K. kingae* generally proceeds as follows: Prepilins have their hydrophilic leader peptide cleaved by the prepilin peptidase PilD, and the mature pilins are inserted into the periplasmic leaflet of the inner membrane by their hydrophobic tail (Strom, Nunn et al. 1994). Pilins are incorporated into the growing pilus by the extension ATPase PilF and are secreted through the outer membrane secretin composed of PilQ subunits (Kehl-Fie, Miller et al. 2008). Additional auxiliary proteins are predicted to

provide rigidity to the machinery and anchor the pilus to the inner membrane and peptidoglycan.

The distinguishing characteristic of T4P is their ability to retract (Merz, So et al. 2000). Retraction is driven by depolymerization of the pilus by the PilT ATPase. Evidence suggests that pilins are retained and reused throughout several cycles of pilus extension and retraction (Skerker and Berg 2001). T4P retraction confers twitching motility to the bacterium (Merz, So et al. 2000). This type of motility involves extension of T4P along a surface, adherence to the surface, and subsequent retraction, thereby dragging the bacterium towards the point of attachment. When viewed by microscopy the bacterium appears to twitch or slingshot along the surface (Skerker and Berg 2001, Jin, Conrad et al. 2011). The retraction ATPase PilT is one of the strongest molecular motors described to date (Maier, Potter et al. 2002, Clausen, Jakovljevic et al. 2009). Pili pulling experiments using *Myxococcus xanthus* have given the forces exerted by T4P retraction to be as high as 149 pN (Clausen, Jakovljevic et al. 2009).

1.3.2 T4P as flexible adhesins

The flexibility of T4P also contributes to resistance of the adhesive bond to shear forces. Nanoscale pulling of T4P in experiments with *Pseudomonas aeruginosa* using AFM revealed that the flexibility of T4P can be described by the worm-like chain (WLC) (Lu, Giuliani et al. 2015). Pulling on a single pilus adhered to several surfaces revealed multiple force peaks and plateaus that indicated that multiple hydrophilic and

hydrophobic interactions occurred along the length of the pilus. The multiple peaks and their relatively low amplitude indicate that adherence to surfaces mediated by T4P is low affinity, but high avidity. The low affinity and high avidity adherence allows single T4P-mediated adherence to resist pulling forces of up to 250 pN (Beaussart, Baker et al. 2014). Furthermore, the helical arrangement of pilins in the pilus allows T4P to act as molecular nanosprings (Beaussart, Baker et al. 2014, Lu, Giuliani et al. 2015). Unravelling of the helix contributes to the resistance of pulling forces by the pilus.

1.4 Trimeric autotransporter adhesins

1.4.1 TAA history

Previously we have demonstrated that the TAA Knh is a major adhesin responsible for tight-adherence to Chang cell monolayers (Porsch, Kehl-Fie et al. 2012, Kern, Porsch et al. 2017). The prototypical TAA is YadA from *Yersinia* species which was originally described to be an important multi-role adhesin contributing to adherence to host cells, invasion, and extracellular matrix protein binding (Bukholm, Kapperud et al. 1990, Viljanen, Lounatmaa et al. 1991, Terti, Skurnik et al. 1992, Bliska, Copass et al. 1993, Tamm, Tarkkanen et al. 1993, Yang and Isberg 1993, Skurnik, el Tahir et al. 1994). YadA was also found to contribute to *Y. enterocolitica* serum resistance (Pilz, Vocke et al. 1992, China, Sory et al. 1993) and to confer *Y. enterocolitica* resistance to antimicrobial peptides (Visser, Hiemstra et al. 1996). Although YadA has been known to be multimeric from the early 1990's (Tamm, Tarkkanen et al. 1993), the structure of folded YadA was not described until 2000 (Hoiczky, Roggenkamp et al. 2000). Hoiczky

et al. described YadA and the related *Moraxella catarrhalis* protein UspA as having a “lollipop” structure, observable via electron microscopy. It was recognized in 2005 that YadA-like proteins represented a novel class of autotransporter proteins, resulting in the designation of trimeric autotransporter proteins (Cotter, Surana et al. 2005).

1.4.2 TAA biosynthesis and structure

TAAAs are characterized by a C-terminal membrane anchor domain composed of four β -sheets that trimerize to form a twelve strand β -barrel pore in the outer membrane of the bacterium (Surana, Cutter et al. 2004). This architecture distinguishes them from conventional autotransporter proteins, which are monomeric. Insertion of the trimerized β -barrel into the outer membrane is known to be BamA dependent (Lehr, Schutz et al. 2010), though the role of BamA in the translocation of the passenger domain remains unknown at this time. Additionally, it has been demonstrated that electrostatic repulsion between positively charged residues projecting into the pore is essential for correct alignment of the monomers within the trimer and therefore stabilizes the trimer (Aoki, Sato et al. 2017).

Trimerization of the β -barrel pore is sufficient for secretion of the N-terminal passenger domain (Mikula, Leo et al. 2012), where it folds and trimerizes to form a rod-like surface structure. Evidence suggests that several periplasmic proteins act either as chaperones to prevent the passenger domain from folding prematurely and/or act to anchor the mature adhesin to the outer membrane (Qu, Mayer et al. 2007, Grin, Hartmann et al.

2014, Ishikawa, Yoshimoto et al. 2016). The mechanism of secretion of the passenger domain to the cell surface remains controversial. It has been shown that the pore produced by TAA trimerization is too small to allow the fully folded passenger domain to pass through. Therefore, it has been proposed by that unfolded passenger domain is translocated either in an N to C-terminal manner (threading model) or C to N-terminal manner (hairpin model) (Oomen, van Ulsen et al. 2004). Alternatively, Oomen and colleagues propose that passenger domains could be translocated via the BamA (Omp85) complex, which has been shown to be involved in classical autotransporter secretion (Voulhoux, Bos et al. 2003). More recently, it has been proposed that BamA complexing with the trimerized translocation domains could hold the pore in a widened state (Lehr, Schutz et al. 2010), which would facilitate passenger domain translocation as has been reported for conventional autotransporters (Dautin and Bernstein 2007).

Although TAAs are a diverse family of proteins, there is strong conservation of passenger domain structural motifs between heterologous passenger domains. A common example is the β -roll structure of the head domain of YadA, which has homologues in many TAAs from other species, including Knh. Structural homologues are frequently identified *in silico* by amino acid sequence homology, such as by the now defunct daTAA server from the Max Planck Institute (Szczesny and Lupas 2008), and TAAs with a YLHD have the classic lollipop structure visible by TEM (Figure 2).

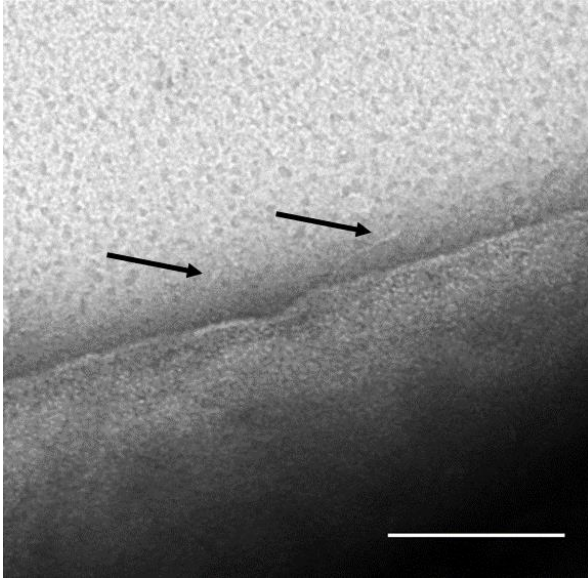


Figure 2. TEM micrograph of Knh (arrows) on the surface of *K. kingae* demonstrating the classic lollipop shape of TAAs containing an N-terminal YLHD. Scale bar is 100 nm. Adapted from Kern et al. 2017.

However, recent crystal structure studies have revealed that there can be variation between *in silico* predictions and crystal structures (Wright, Thomsen et al. 2017). Wright et al. (2017) crystallized the putative domain 1 of the *H. influenzae* Hsf protein and found that the domain contained an additional N-terminal TRP ring in addition to the predicted motifs giving the domain a novel N-TRPring:KG:TRPring-C conformation. Crystallization studies were also key in determining the non-canonical “head” structure of NadA from serogroup B *Neisseria meningitides* (Malito, Biancucci et al. 2014) which consists of a short coiled-coil segment followed by β -sheet “wings” that fold up towards the N-terminus. Similarly, *Bartonella henselae* BadA was shown to have a novel head domain, which consists of a short YLHD followed by two β -prism domains with no homology to known TAA structures (Szczesny, Linke et al. 2008), although there is

some resemblance to domains from the *H. influenzae* Hia TAA in permuted order. These examples highlight the caution with which homology based structural predictions must be treated.

1.4.3 TAA adhesive activities

All TAAs characterized to date have been shown to have adhesive activities. Common targets include integrins, glycoproteins, extracellular matrix proteins, and soluble complement factors (Lyskowski, Leo et al. 2011). Several TAAs are also known to have roles in autoaggregation and biofilm formation (Lazar Adler, Dean et al. 2013, Wang, Hsieh et al. 2014, Wang, Qin et al. 2015). There is some information regarding the relationship between the structure and function of TAAs. Two of the best studied examples are Hia/Hsf from *H. influenzae* and BadA from *B. henselae*.

Hia is expressed by non-typeable (nonencapsulated) *H. influenzae* (NtHi) strains, while Hsf is expressed by encapsulated *H. influenzae*. It has been shown that the two binding domains (BD) of Hia and Hsf, are characterized by a repeating motif of a TRP ring immediately followed by a downstream IS Neck (Laarmann, Cutter et al. 2002, Cotter, Surana et al. 2005). However, despite the evidence that in Hsf BD1 and BD2 mediate adherence to host cells, only BD2 has significant adhesive activity to vitronectin. Vn binding by Hsf BD2 has been shown to contribute to serum resistance by strains expressing Hsf (Singh, Su et al. 2014), which is hypothesized to partially explain why Hsf expressing strains are more often associated with invasive disease.

Similarly, the head region and stalk region of *B. henselae* BadA have been shown to have both overlapping and differential adhesive properties to ECM proteins (Kaiser, Linke et al. 2012). Specifically, the head region and stalk both bind collagen and mediate adherence to host cells, but only the stalk binds to fibronectin. Furthermore, only four of the twenty-three stalk repeats are required for adherence to host cells.

1.4.4 Intraspecies TAA variability

As mentioned previously, there is a large amount of interspecies diversity among TAAs. There can also be significant intraspecies sequence diversity. *H. influenzae* strains encode a rich diversity of TAAs. The aforementioned Hia and Hsf can be considered variants of each other. They have a significant amount of identity and similarity, particularly in the binding domains BD1 and BD2, and absolute identity in the C-terminal membrane anchor (Cotter, Surana et al. 2005). Other *H. influenzae* biogroups as well as other *Haemophilus* species produce TAAs with significant variation. *H. influenzae* biogroup *aegyptius* encodes the *tab/tah* family of TAAs, alleles of which are lineage specific (Strouts, Power et al. 2012). Pathogenic *H. parasuis* strains encode 13 paralogous TAAs of the VtaA family divided into three groups by homology (Pina, Olvera et al. 2009). VtaA variants from all three groups have homologs in nonpathogenic strains; however, microarray assays have demonstrated that these variants have significant divergence from the pathogenic strains.

The variation of NadA from *Neisseria meningitidis* has been characterized in some depth (Comanducci, Bambini et al. 2004, Bambini, De Chiara et al. 2014). Generally, the six enumerated alleles are grouped into two groups (I and II) based on sequence homology (Bambini, De Chiara et al. 2014). Group I alleles are associated with pathogenic strains and the hypervirulent clonal complexes, while group II alleles are largely associated with carrier isolates. Within each group, alleles display 80-99% homology; however, between the two groups, there is only 40-50% homology (Bambini, De Chiara et al. 2014). This variation has been shown to influence antibody reactivity against NadA, with antibodies made against group I variants not having crossreactivity to group II variants (Malito, Biancucci et al. 2014).

1.4.5 TAAs as flexible adhesins

Similar to T4P, TAAs have been shown to be flexible and to act as molecular springs (El-Kirat-Chatel, Mil-Homens et al. 2013, Koiwai, Hartmann et al. 2016). This flexibility allows TAA-mediated adherence to resist pulling forces. Unlike T4P, AFM pulling experiments revealed that TAAs act as linear springs. Force curves generated in AFM experiments revealed force is proportional to distance, rather than being fit by the worm-like chain model, and had short bond rupture distances of ~50 nm (El-Kirat-Chatel, Mil-Homens et al. 2013). This property indicates that TAAs do not unfold when pulled, but rather act as stiff rod-like springs. The structural basis for the flexibility of TAAs stems from the ability of a variety of structural domains to allow for several degrees stalk

bending each, resulting in a net maximal degree of flexibility of 90° in the case of AtaA from *Acinetobacter* sp. strain Tol 5 (Koiwai, Hartmann et al. 2016).

1.5 Models of shear stress and bacterial adherence

Much of the work describing bacterial adherence to surfaces and host cells has been done under static conditions such as those found in tissue culture plates. However, many physiological niches feature liquid flow, which exerts shear forces on adherent bacteria. Mucociliary clearance in the pharynx, blood flow in the vascular system, and voiding of urine in the urinary tract represent just a few of the niches where shear stress is experienced by the bacterium. Therefore, study of bacterial adherence under shear stress is important.

Several models of bacterial adherence under shear stress have been developed. One of the earliest models used to study bacterial adherence is the radial flow chamber in which liquid is flowed between two disks from a central point (Duddridge, Kent et al. 1982, Nagel, Dickinson et al. 1996). The shear stress experienced by bacteria or cells within the apparatus varies proportionally to the distance from the center of the disk; therefore, adherence can be studied at a continuous range of shear stress (Duddridge, Kent et al. 1982).

A model of bacterial adherence under shear stress currently commonly found in the literature is assessment of adherence using linear flow chambers. In these assays, buffer or inoculum is pumped into the chamber at one end. The chamber can be prepared with host cells, adherent bacteria or biofilms, or can be functionalized with coatings, such as with purified receptor proteins. The spent inoculum or buffer flows out the opposite end of the chamber into waste or, as in the variations using a peristaltic pump, can be recirculated. These assays allow for very precise control of the shear forces experienced by bacteria at the chamber walls. These assays have been used to examine initial bacterial attachment (Nejadnik, van der Mei et al. 2008, Szlavik, Paiva et al. 2012), persistence of adherence under shear stress (Niddam, Ebady et al. 2017, Oder, Fink et al. 2017), and biofilm formation (Cook, Costerton et al. 1998, Thomen, Robert et al. 2017). Recently, *ex vivo* models of bacterial adherence under shear stress have been developed (Weidensdorfer, Chae et al. 2015, Veloso, Claes et al. 2018). These models vary from using graft sections in flow chambers (Veloso, Claes et al. 2018) to flowing bacteria through sections of human umbilical cord (Weidensdorfer, Chae et al. 2015).

1.6 Model of *K. kingae* adherence to host cells

In previous work, our lab demonstrated that *K. kingae* expresses three surface factors that either mediate or modulate adherence to host cells *in vitro*: type IV pili, the TAA Knh, and a polysaccharide capsule. Using standard static adherence assays to examine the adherence of mutants of T4P, Knh, and capsule individually and in combination (Porsch, Kehl-Fie et al. 2012). Elimination of T4P resulted in a strain unable to adhere

to Chang cells, but further elimination of the capsule restored wild type adherence. A T4P and Knh double mutant strain and a T4P, Knh, and capsule triple mutant strain were non-adherent. This information suggests that T4P and Knh are the major adhesins involved in *K. kingae* to host cells and that capsule can inhibit Knh-mediated adherence when T4P are absent. Furthermore, a T4P retraction deficient mutant mediated an intermediate level of adherence similar to a Knh/capsule double mutant.

Taken together, these results suggest that Knh mediates a higher level of adherence than T4P and that T4P retraction is necessary to overcome capsular inhibition of Knh-mediated adherence. We hypothesized that *K. kingae* adheres according to the following model (Figure 3): The T4P projecting beyond the capsule make initial contact with the host cell and mediate low affinity adherence. T4P then retract, drawing the organism closer to the host cell and causing the displacement of capsule, which exposes Knh to the host cell surface allowing Knh to mediate tight adherence to the host cell. This model represents a novel mechanism for modulating the activity of a TAA via the presence of a polysaccharide capsule.

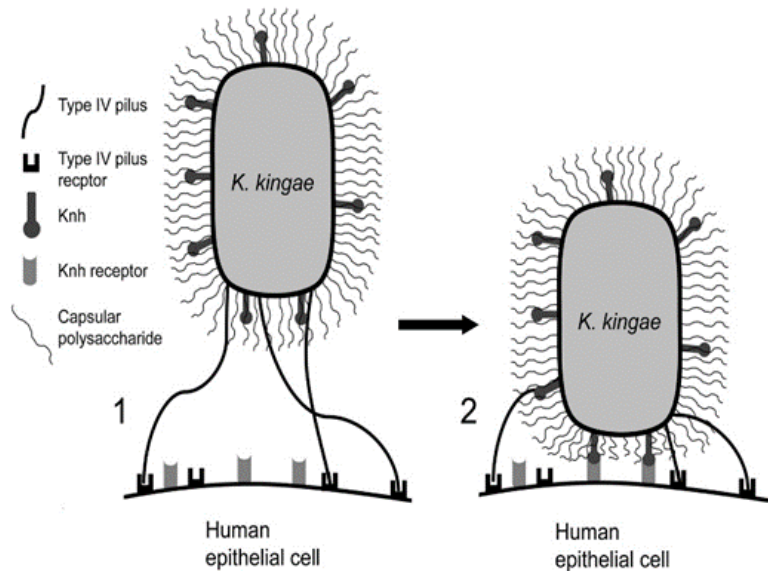


Figure 3. Model of *K. kingae* adherence to host cells. 1. T4P make initial contact with the host cell and mediate low affinity adherence. 2. T4P retract, drawing the organism closer to the host cell and causing capsule to be displaced, which allows Knh to access the host cell surface and mediate tight adherence. Adapted from Porsch et al. 2012.

1.7 Dissertation overview

Chapter 2 defines the mechanical features of our model, including a comparison of Knh and T4P-mediated adherence under shear stress, measurements of the depth of capsule, and the requirement of T4P retraction under shear stress. Chapter 3 examines the sequence variability of Knh between clinical isolates as well as the variation in adhesive activities of select Knh variants. Finally, chapter 4 summarizes our findings and proposes potential future directions.

Chapter 2: Defining the mechanical determinants of *Kingella kingae* adherence to host cells

2.1 Introduction

Adherence to host epithelial cells is an important first step in the colonization of a host by potential bacterial pathogens. *Kingella kingae* is a pediatric pathogen that colonizes the posterior pharynx of young children (Yagupsky 2004). Improved culture methods and PCR-based detection methods have revealed that *K. kingae* is a leading etiology of osteoarticular infections among children in this age group in an increasing number of countries (Gene, Garcia-Garcia et al. 2004, Chometon, Benito et al. 2007, Ceroni, Cherkaoui et al. 2010, Yagupsky, El Houmami et al. 2017). Analysis of paired clinical isolates from the oropharynx and the site of invasive disease in pediatric patients has demonstrated that invasive disease likely proceeds from pharyngeal colonization. Approximately 10% of young children are colonized at a given time, and roughly 70% of children are colonized at some point during the first 48 months of life (Yagupsky, Dagan et al. 1995, Slonim, Walker et al. 1998, Yagupsky, Peled et al. 2002).

Previous work by our group has demonstrated that *K. kingae* adherence to human epithelial cells is influenced by three surface factors: type IV pili (T4P), a trimeric autotransporter adhesin (TAA) called *Kingella NhhA* homologue (Knh), and a polysaccharide capsule (Porsch, Kehl-Fie et al. 2012). T4P are long surface fibers that consist of polymers of pilin subunits and are distinguished from other pilus types by their

ability to undergo retraction. These fibers confer a type of motility termed twitching motility, in which T4P extend, adhere to a surface, and then retract, dragging the bacterium forward (Skerker and Berg 2001). TAAs comprise the type Vc autotransporter family of bacterial surface proteins and are characterized by a homotrimeric architecture (Lyskowski, Leo et al. 2011). Every TAA examined to date has demonstrated adhesive activities, either promoting bacterial adherence to host molecules or abiotic surfaces or binding circulating factors such as immunoglobulins and complement components (Lyskowski, Leo et al. 2011). Capsules consist of long polysaccharide chains anchored to the outer membrane via a lipid moiety (Whitfield 2006). In a variety of bacteria, capsules have been shown to be important virulence factors associated with immune evasion (Hallstrom and Riesbeck 2010, Hill, Griffiths et al. 2010, Miajlovic and Smith 2014).

In previous studies, T4P, Knh, and capsule have been examined for their contributions to *K. kingae* adherence to host cells using standard static adherence assays with fixed Chang cell monolayers (Kehl-Fie, Miller et al. 2008, Porsch, Kehl-Fie et al. 2012). Deletion of the gene encoding the T4P major pilin subunit *pilA1* results in elimination of pili and abolishes adherence. Concomitant inactivation of the capsule transport gene *ctrA* eliminates encapsulation and restores adherence to wild-type levels. Inactivation of the *knh* gene encoding Knh or the *pilT* gene encoding the T4P retraction ATPase PilT results in an intermediate level of adherence to host cells when capsule is present. A strain deficient in both T4P and Knh is non-adherent, regardless of encapsulation state.

Our earlier observations of T4P-mediated and Knh-mediated adherence to host cells and the effects of capsule on this adherence suggested three hypotheses: Knh mediates stronger adherence than do T4P; capsule is deeper than Knh is long and interferes with Knh-mediated adherence; capsule displacement and intimate Knh-mediated adherence requires PilT-driven T4P retraction. In the present study we sought to address these hypotheses, ultimately elucidating the mechanical determinants of *K. kingae* adherence to host cells.

2.2 Results

***K. kingae* Knh-mediated adherence is stronger than T4P-mediated adherence in the setting of shear stress.** To study the relative levels of adherence mediated by Knh and T4P, we used a dynamic flow system to apply shear stress to bacteria after the bacteria had been pre-anchored to host cells under static conditions and on initial contact with host cells. For assays comparing Knh-mediated adherence and T4P-mediated adherence, we used non-encapsulated KK01-derived strains expressing either only T4P (KK01 *knhctrA*), only Knh (KK01 *pilA1ctrA*), or neither T4P nor Knh (KK01 *pilA1knhctrA*). Representative images are included in Figure S1. To test the ability of Knh and T4P to anchor the bacterium to the host cell under shear stress we used the shear resistance adherence (SRA) assay (Figure 1A) in which bacteria are pre-adhered to host cell monolayers and non-adherent bacteria are washed away with buffer under constant shear stress. We observed that Knh mediated high-level adherence and T4P mediated low-level adherence at all shear stress rates tested (Figure 1B). Both Knh and T4P mediated lower adherence at low shear stress and higher adherence at high

shear stress. Strain KK01*pilA1ctrA* had an adherence level of ~11 bacteria/cell at 0.1 dyne, increasing to ~42 bacteria/cell at 5 dyne, and then decreasing to ~31 bacteria/cell at 15 dyne. In contrast, strain KK01*knhctrA* had an adherence level of ~5 bacteria/cell at 0.1 dyne, increasing steadily to ~25 bacteria/cell at 15 dyne. Adherence by strain KK01*pilA1ctrA* was significantly higher ($p < 0.05$) than adherence by strain KK01*knhctrA* at all shear stress levels except 15 dyne ($p = 0.28$). A control strain KK01*pilA1knhctrA* had an average of < 1 bacteria/cell at all shear stress levels. These results indicate that Knh-mediated adherence is stronger than T4P-mediated adherence while under shear stress.

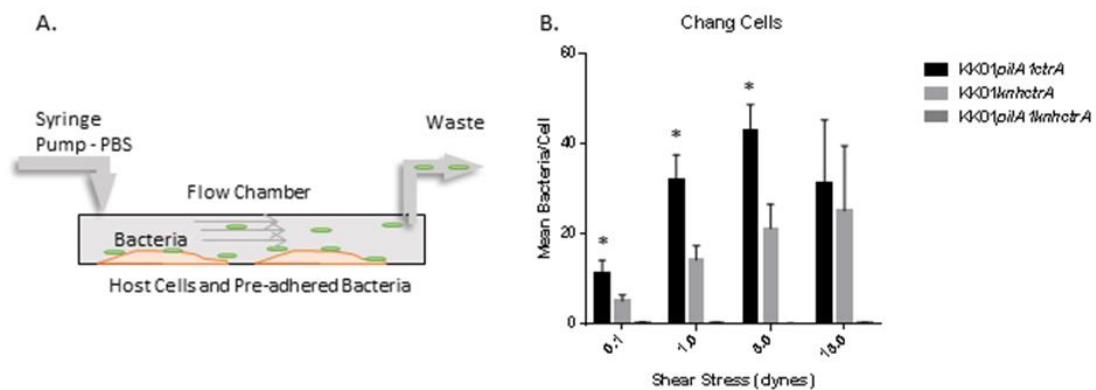


Figure 1. Shear resistance adherence (SRA) assays. A) Schematic of SRA assays. Host cell monolayers are infected with bacteria under static conditions, and non-adherent bacteria are washed away with PBS under constant shear stress. B) Adherence of Knh-mediated (KK01*pilA1ctrA*) and T4P-mediated (KK01*knhctrA*) adherence to fixed Chang cell monolayers under shear stress. Strain KK01*pilA1knhctrA* was used as a negative control. Error bars represent standard deviation. Strain KK01*pilA1ctrA* was significantly more adherent than KK01*knhctrA* at the shear rates of 0.1, 1.0, and 5.0 dynes ($*p < 0.05$), and strain KK01*knhctrA* was more adherent than strain KK01*pilA1knhctrA* at all shear rates ($p < 0.05$).

To test the ability of *K. kingae* to adhere on initial contact, we developed the inoculating under shear adherence (ISA) assay (Figure 2A) in which bacteria resuspended in buffer are flowed over host cell monolayers under constant shear stress. This assay revealed that *Knh* mediated significantly higher level adherence to host cells on initial contact than did T4P (Figure 2B). At a shear stress of 0.1 dyne, we observed that strain KK01*pilA1ctrA* had a mean adherence level of nearly 12 bacteria/cell. Although there was a sharp decrease in KK01*pilA1ctrA* adherence to 6 bacteria/cell at 0.2 dyne, adherence remained between 4 and 6 bacteria/cell until 2 dynes and decreased to ~2 bacteria/cell at 5 dynes. In contrast, strain KK01*knhctrA* had a mean adherence level of only 2 bacteria/cell at 0.1 dyne and negligible adherence at 0.3 dyne. At shear stress rates higher than 15 dynes, the Chang cell monolayer began to lose integrity, precluding examination of higher shear stress. To confirm our results, we repeated the ISA assays with A549 cell monolayers at select shear levels up to the shear level at the adherence plateau noted with Chang cells (Figure 2C). Although overall adherence to A549 cells by both KK01*pilA1ctrA* and KK01*knhctrA* was slightly reduced compared with adherence to Chang cells, the relationship between KK01*pilA1ctrA* and KK01*knhctrA* adherence remained the same.

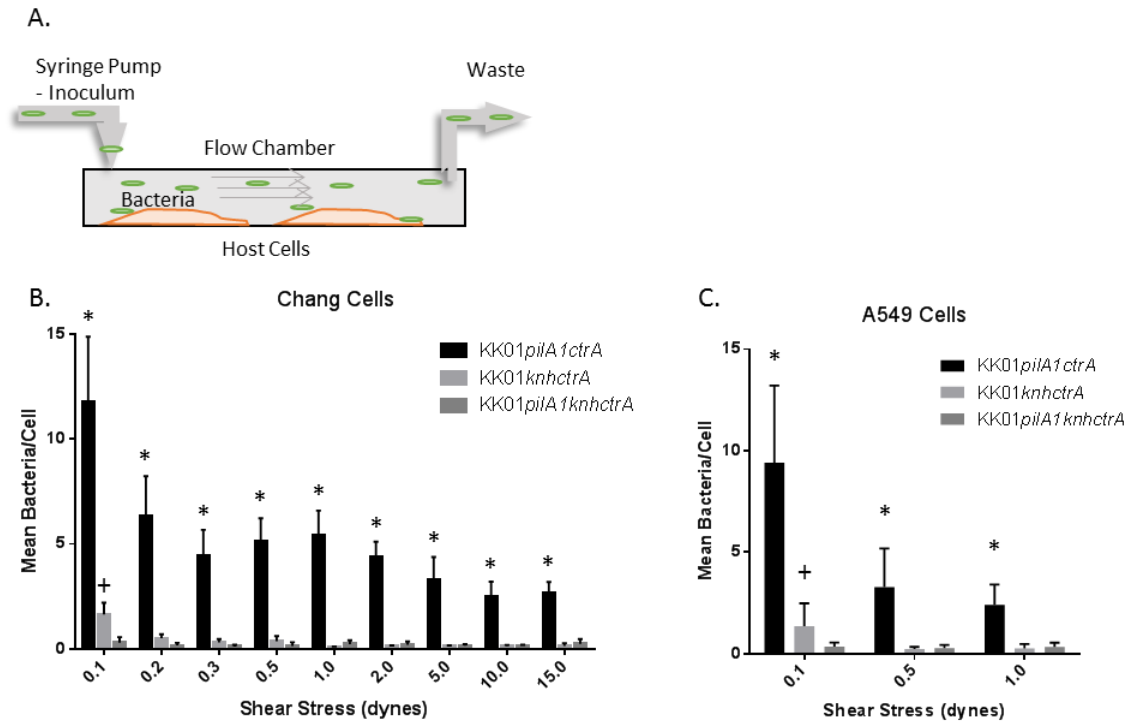


Figure 2. Inoculating under shear adherence (ISA) assays. A) Schematic of ISA assays. Suspensions of bacteria are flowed over host cell monolayers under constant shear stress. B) *Knh* (KK01*pilA1ctrA*) and T4P (KK01*knhctrA*) ISA adherence to fixed Chang cell monolayers and C) fixed A549 cell monolayers. Error bars represent standard deviation. Adherence by strain KK01*pilA1ctrA* was significantly higher than adherence by strain KK01*knhctrA* at all shear rates (* $p < 0.05$), and KK01*knhctrA* was significantly more adherent than strain KK01*pilA1knhctrA* only at 0.1 dyne only for both Chang cells and A549 cells (+ $p < 0.05$).

Atomic force microscopy reveals that the *K. kingae* capsule is approximately 700 nm deep. To determine the depth of the capsule of strain KK01, we measured the resistance of the bacterial surface to indentation using atomic force microscopy (AFM) (Figure 3A). We gathered single point force curves for individual bacteria, using the nonencapsulated strain KK01*ctrA* as a control. We fit Hooke's law to the area of linear

compliance, which corresponds to the resistance of the bacterium body. The depth of capsule was defined as the Z distance between the initiation of the probe tip deflection and the beginning of linear compliance fit by Hooke's law. Analysis of the force curves using this method revealed that the *K. kingae* capsule of strain KK01 was 700 nm deep on average (n=20, range=300-900 nm).

Knh fibers are ~110 nm long. Using negative staining TEM, we were able to visualize Knh fibers on the surface of bacteria. Given that *K. kingae* strain KK01 expresses relatively little Knh, we examined strain KK03, a variant of KK01 that expresses high quantities of Knh (Figure S2). To ensure that the only surface structures visualized were Knh, we examined strain KK03*pilA1ctrA* (lacking T4P and capsule) (Figure 3B), using strain KK03*pilA1knhctrA* (lacking Knh, T4P, and capsule) as a control (Figure 3C). The observed fibers ranged in length from 46 nm to 112 nm (mean length=68 nm, standard deviation=14 nm, n=92), likely reflecting the curvature of some fibers and the partial obscuring of the base of some fibers related to the 2-dimensional nature of TEM. Fibers were absent on the surface of strain KK03*pilA1knhctrA*.

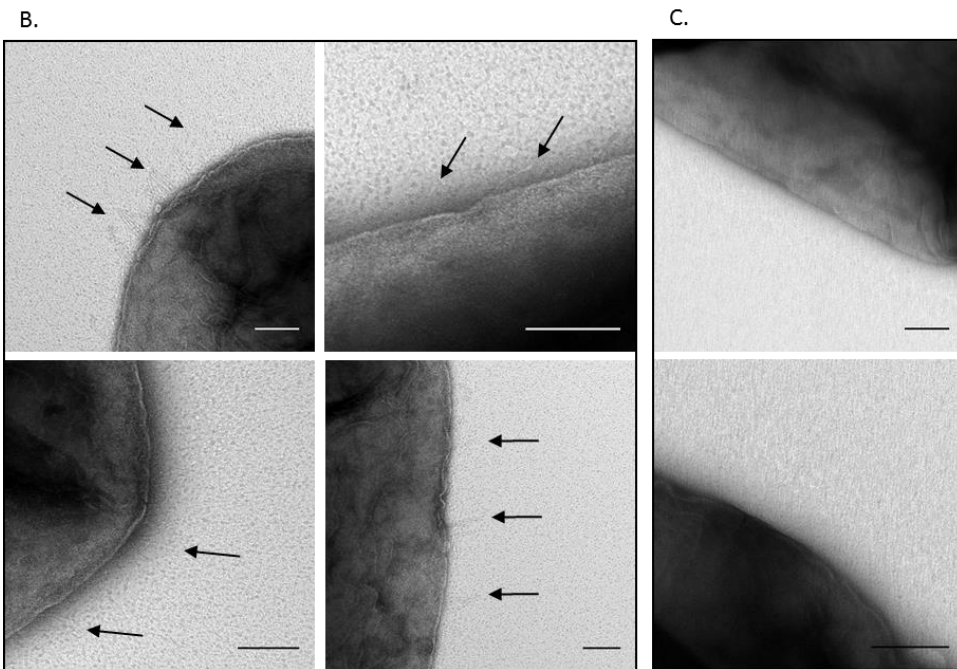
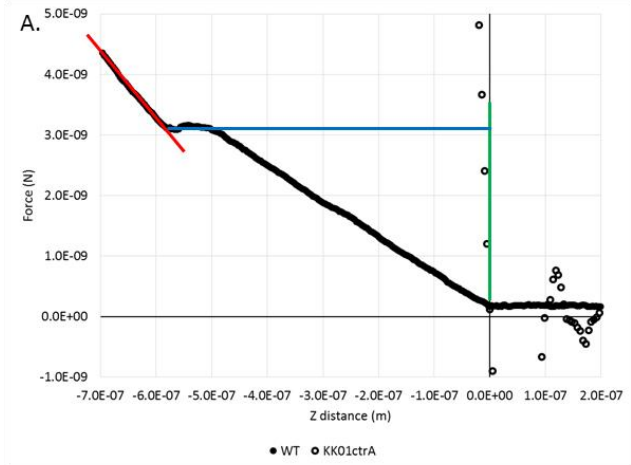


Figure 3. Depth of *K. kingae* capsule versus Knh length. A) Example AFM single point force curve of strain KK01 (solid circles). The green line indicates the beginning of tip deflection. The red line is the linear regime corresponding with the resistance of the bacterial membrane. The blue line represents the distance of capsule indentation. Included is an example force curve from the nonencapsulated strain KK01ctrA (open circles). Transmission electron micrographs of *K. kingae* surface fibers using uranyl acetate negative staining of B) the KK03pilA1ctrA mutant and C) the KK03pilA1knhctrA mutant. Knh fibers are marked with arrows. Scale bar represents 100 nm.

Capsule is displaced on bacteria in close contact with host cells. To visualize the bacterial capsule, we stained Chang cell monolayers infected with strains KK01 and KK01 *pilT* (which expresses non-retractile T4P) with cationic ferritin, resulting in an electron dense layer that was visible on the bacterial cell surface when examined by thin section TEM. With each sample, we observed four grids and at least 40 bacteria per grid. When wild-type bacteria were in close contact with host cells, we observed that the capsule was consistently thinner between the bacterium and the host cell (Figure 4A). In contrast, the capsule of strain KK01 *pilT* (Figure 4B) remained similar in depth to the capsule of nonadherent bacteria (Figure 4C), even when the bacteria were in close contact with host cells.

T4P retraction increases the level of adherence to host cells of an encapsulated strain under shear stress. To test the contribution of T4P retraction to adherence, we compared strain KK01 with mutants lacking PilT (KK01 *pilT*) or lacking Knh (KK01 *knh*) in SRA assays, using strain KK01 *pilA1knh* as a control (Figure 4D). We found that the level of adherence was significantly higher for strain KK01 than for the KK01 *pilT* mutant at all levels of shear stress ($p < 0.05$). The KK01 *pilT* mutant had a similar level of adherence as the KK01 *knh* mutant, in agreement with our static adherence assay results (Porsch, Kehl-Fie et al. 2012), while the KK01 *pilA1knh* double mutant control had minimal adherence.

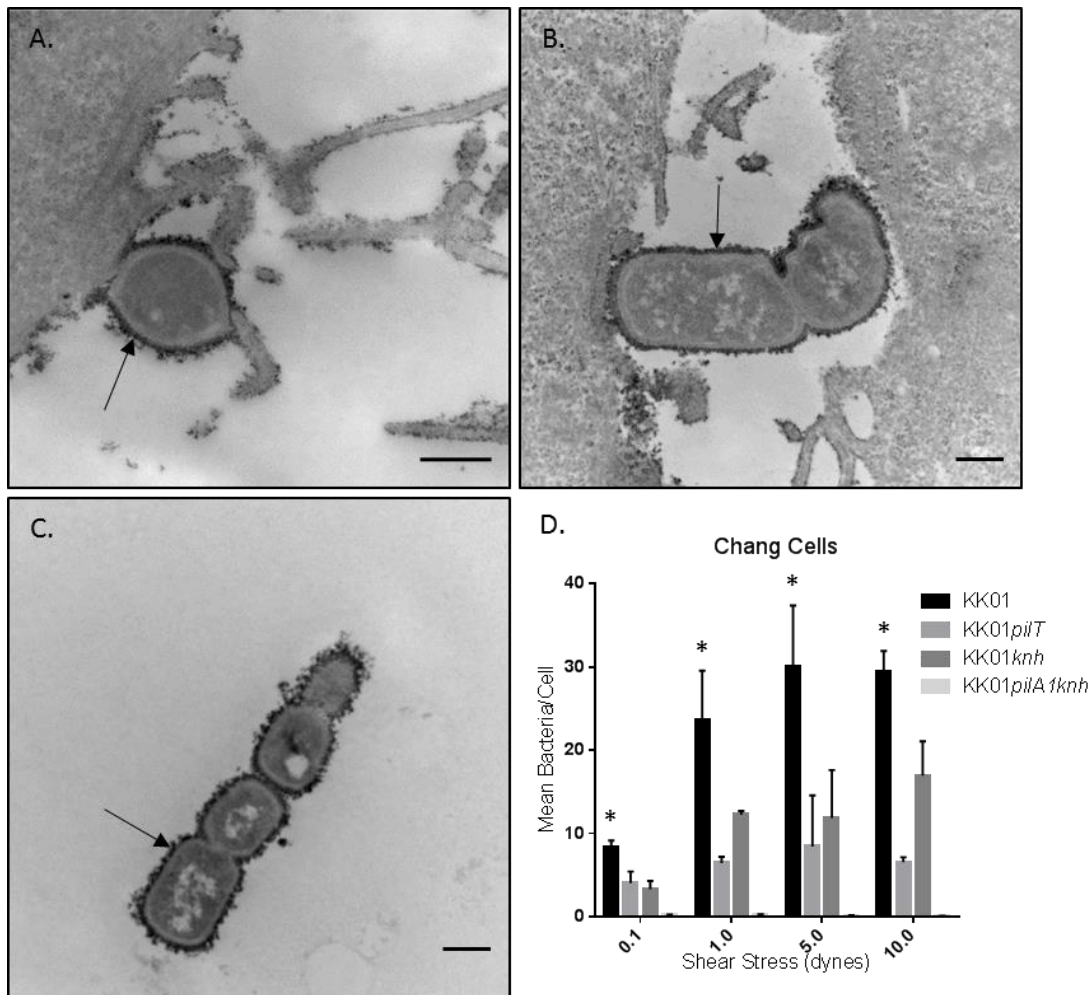


Figure 4. Capsule displacement and T4P retraction. Thin section TEM micrographs of A) wild type KK01 and B) the KK01*pilT* mutant in close contact with host Chang epithelial cell membranes and microvilli. The capsule is stained with cationic ferritin and appears as an electron dense layer around the bacterium (arrows). Scale bars represent 500 nm. C) A wild type KK01 bacterium not in close contact with a host cell. D) SRA assay comparing the adherence of wild type KK01, the KK01*pilT* mutant, and the KK01*knh* mutant. Strain KK01*pilA1knh* was used as a negative control. Error bars represent standard deviation. KK01 adhered at a significantly higher rate than strains KK01*pilT* and KK01*knh* at all shear levels (* $p < 0.05$).

2.3 Discussion

In previous work we described the relationship between T4P, the trimeric autotransporter adhesin Knh, and capsule in *K. kingae* adherence to host cells (Porsch, Kehl-Fie et al. 2012). This earlier work suggested a novel model of adherence and generated three hypotheses: 1) Knh mediates stronger adherence to host cells than do T4P; 2) the capsule of *K. kingae* is deeper than Knh is long; 3) T4P retraction causes capsule displacement and is necessary for Knh-mediated adherence.

To examine whether Knh mediates stronger adherence than do T4P, we used flow adherence assays and examined adherence under shear stress. The ideal method to quantitate the binding affinity of an adhesin to its receptor involves assessment of binding of the purified adhesin to the purified receptor in an enzyme-linked immunosorbent assay (ELISA) or surface plasmon resonance. However, purification of the adhesive passenger domain of Knh has proven to be challenging, and the receptor for Knh and T4P remains unknown. We reasoned that examination of bacterial adherence under shear stress would be an alternate approach to compare the adherence properties of Knh and T4P. Adherence under shear stress assays have the advantage that the adhesins are expressed in their native context, making adhesin folding, glycosylation (Rempe, Spruce et al. 2015), stability, and orientation of minimal concern. A potential limitation of flow adherence assays is the difficulty of separating the contributions of affinity and avidity, related to multivalent adhesive activities. However, because our interest is the adherence properties of the whole bacterium to a host cell, this limitation also represents a strength.

Typically, adherence assays performed under shear stress have used flow chambers that are pre-inoculated with bacteria under static conditions or very low shear (Kaiser, Linke et al. 2012). Subsequently, buffer is flowed through the chambers to wash away non-adherent bacteria. We have called these assays shear resistance adherence (SRA) assays, as they measure the ability of the adhesin to anchor the bacterium to the host cell after maximal contact between the bacterium and the host cell has been achieved. Additionally, we were interested in the level of adherence on initial contact by the bacteria to host cells, reasoning that initial contact of the bacterium to a host cell occurs under a variety of shear conditions *in vivo*. Therefore, we also performed experiments in which the inoculum was flowed through the flow chambers over the host cell monolayers. We have called these assays inoculating under shear adherence (ISA) assays. Data are lacking regarding the shear forces within the liquid or mucosal layer of the upper respiratory tract, but the shear exerted by airflow in the respiratory tract at the mucosal surface is reported to be 0.5-2 dynes (Green 2004).

The results of both the SRA and ISA assays demonstrated that Knh-mediated adherence can withstand significantly higher shear stress than can T4P-mediated adherence and that Knh mediates adherence more frequently on initial contact. These results strongly suggest that Knh mediates stronger bacterial adherence than do T4P, whether as a consequence of greater affinity or greater avidity or both.

Interestingly, in SRA assays Knh and T4P generally demonstrated increasing adherence as shear stress increased. Although counterintuitive, this phenomenon has been noted before with other adhesins and has been best studied with FimH and various pilus components expressed by *E. coli*. (Thomas, Trintchina et al. 2002, Thomas, Nilsson et al. 2004) The positive relationship between shear stress and adherence by flexible fibrous adhesins has been attributed to conformational changes in the fiber or adhesin induced by shear stress, resulting in increased affinity for the receptor and/or buffering of the adhesive bond from environmental shear stress (Beaussart, Baker et al. 2014, Lu, Giuliani et al. 2015). This mechanism has been proposed to enable adherent bacteria to resist peeling forces under high shear situations. TAAs have been shown to have significant flexibility (El-Kirat-Chatel, Mil-Homens et al. 2013, Koiwai, Hartmann et al. 2016), although few studies have specifically examined the contribution of TAA flexibility to affinity. Our observations of Knh by TEM revealed fibers with significant amounts of curvilinearity, strongly suggesting that Knh is flexible and supporting the possibility that Knh flexibility contributes to affinity.

Our earlier work demonstrated that T4P observed by TEM are typically several microns long and would clearly extend beyond the capsule, allowing them to make initial contact with host cells (Kehl-Fie, Miller et al. 2008, Porsch, Kehl-Fie et al. 2012). Furthermore, T4P conferred twitching motility to the bacterium, a hallmark of T4P retraction (Porsch, Kehl-Fie et al. 2012). This earlier work also suggested that capsule masks Knh and inhibits Knh-mediated adherence until T4P retraction causes capsule to be displaced and Knh to be exposed to the host cell (Porsch, Kehl-Fie et al. 2012). The present work

provides more direct evidence for this mechanism. Measurements of the capsule depth by AFM and of the length of Knh by TEM demonstrated that capsule is deeper than Knh is long. We noted that the depth of capsule observed by AFM is significantly deeper than the apparent depth when cationic ferritin-stained capsule is observed by TEM. We attribute this discrepancy to the fixation conditions of cationic ferritin-staining and embedding for TEM, which have been shown to dehydrate bacterial capsules and lead to the collapse of capsular structures (Stukalov, Korenevsky et al. 2008). The effect of dehydration on capsules makes it difficult to obtain accurate measurements by TEM. Because AFM can be performed with live bacteria in an aqueous environment, capsule remains hydrated and is therefore at its maximal potential depth.

TEM imaging of bacteria in close contact with host cells with cationic ferritin stained capsule showed a very thin or absent layer between the bacterium and host cell with the wild type strain, suggesting that capsule is, in fact, displaced when bacteria adhere to host cells. The cationic ferritin staining between the host cells and bacteria remained the same as on nonadherent bacteria when a strain lacking the T4P retraction ATPase PilT was examined, further supporting the conclusion that T4P retraction is necessary for capsule displacement and ultimately for Knh-mediated adherence.

We performed a second series of SRA assays to assess the contribution of T4P retraction to adherence when capsule is present. We observed that wild type encapsulated strains with retractile T4P had an increased level of adherence compared

to a *pilT* retraction-deficient mutant. The level of adherence by the *pilT* mutant was similar to that of a *knh* mutant. Since a *knh* mutant only adheres via T4P, this observation indicates that a *pilT* strain is also adhering only via T4P. The increased adherence of KK01 is likely due to T4P retraction enabling Knh to mediate high affinity adherence despite the presence of capsule. Others have shown that capsule-deficient strains have increased adherence, biofilm formation, and hemagglutination, but lower virulence (Misawa, Kelley et al. 2015, Tu, Hsieh et al. 2015). However, our observations of capsule depth versus Knh length and capsule displacement leading to increased adherence to host cells provide the first description of capsule displacement as a mechanism leading to intimate bacterial adherence to host cells.

In summary, in this study we have illuminated the mechanisms underlying *K. kingae* adherence to host cells. We observed that Knh mediates adherence at a higher level than T4P under shear stress, suggesting that Knh is capable of mediating stronger adherence to the host cell. Additionally we established that capsule displacement is driven by T4P retraction and results in Knh-mediated adherence.

2.4 Materials and Methods

Strains and culture conditions

The *K. kingae* strains and mutants used in this study are listed in Table 1. KK01 is a stable lab adapted derivative of clinical isolate 269-492 (Kehl-Fie and St Geme 2007). Bacteria were grown from frozen stocks on Chocolate II agar (BD, San Jose, CA) for 16-

17 hours and then were resuspended for use in various assays. Deletions of *pilA1* (Kehl-Fie, Miller et al. 2008), *knh* (Porsch, Kehl-Fie et al. 2012), *ctrA* (Porsch, Kehl-Fie et al. 2012), and *pilT* (Porsch, Kehl-Fie et al. 2012) in *K. kingae* strains were made as describe previously . Elimination of T4P, Knh, or capsule has no effect on the relative quantities of the remaining factors. All strains used had comparable colony forming units per ml at equal OD readings.

Adherence assays under shear

To quantify the level of *K. kingae* adherence to host cells under shear stress, we used a modified bacterial flow adherence assay protocol. Chang cells (ATCC# CCL-20.2) and A549 respiratory cells (ATCC# CCL-185) were maintained in MEM supplemented with 10% FBS and 5% NEAA and MEM supplemented with 10% FBS, respectively, at 37°C in 5% CO₂. One day prior to assays, host cells were seeded into the flow chambers of a μ -slide VI^{0.4} (Ibidi, Germany), allowing them to be approximately 90% confluent at the time of the assay. All adherence assays were performed using host cell monolayers that were fixed using 2% glutaraldehyde in 0.1 M sodium phosphate buffer (pH 7.4), incubated at 4°C for two hours with gentle agitation, and then washed three times with TBS, stabilizing them against the effect of the *K. kingae* RTX toxin.

To test the anchoring of bacteria to host cells by T4P and Knh, we used a shear resistance adherence (SRA) assay as follows (Figure 1A): Bacteria were resuspended in PBS to an OD₆₀₀ of 0.8. Flow chambers containing confluent and fixed host cell

monolayers were infected by aspirating the final TBS wash and adding 40 μ l of the resuspended bacteria. The slides were then gently centrifuged at 165 x g for 5 minutes to settle the bacteria onto the monolayers. Using a syringe pump (Harvard Apparatus, Holliston, MA) with a 10 ml syringe, 5 ml of PBS was flowed through the chambers at a constant flow rate to wash away nonadherent bacteria. Flow rates were converted to shear stress using the conversion table provided by Ibidi (Application Note 11, v4.1). The infected chambers were gently washed once with PBS and then stained using a Three Step Stain Set (Richard-Allan Scientific, Kalamazoo, MI), which is a Giemsa stain kit. Frames of the infected monolayers were captured on a DMIL LED microscope (Leica, Germany) at 40x equipped with a MC120 HD camera (Leica) using LAS 3.4 software (Leica) with a 2x digital zoom. We imaged 5 fields from each chamber, and the total number of adherent bacteria was divided by the total number of cells to give the mean adherent bacteria/cell for each chamber. These assays were performed in triplicate, and the results were reported as shear stress vs. mean bacteria/cell. Significance was determined by Student's t-test.

To test the ability of bacteria to mediate adherence to host cells on initial contact, we performed what we have termed inoculating under shear adherence (ISA) assays (Figure 2A). Bacteria were resuspended in PBS to an OD₆₀₀ of 1.0, diluted 1:2 in PBS, and loaded into 10ml syringes. Using a syringe pump, 5 ml of the inoculum was pumped through flow chambers of the μ -slide VI^{0.4} containing fixed host cell monolayers at a constant flow rate. The chambers were then stained as described above, and the cells

and remaining bacteria were counted and reported as shear stress vs. mean bacteria/cell. Significance was determined by Student's t-test as before.

Atomic force microscopy

To measure the depth of capsule, atomic force microscopy (AFM) was performed as described by Mularski et al. 2016 (Mularski, Wilksch et al. 2016) with some modification. Coverslips or slides were cleaned using glacial acetic acid, washed thoroughly by flooding with diH₂O and then methanol, and allowed to air dry. A 1.0% solution of polyethyleneimine (PEI) in diH₂O was spread on the slides and allowed to sit for 4 hours before washing by flooding with diH₂O and then air drying. Bacteria were resuspended in PBS, and 100 µl of the suspension was placed on the PEI-coated slides. Bacteria were allowed to absorb onto the slides for 1 hour, and the slides were gently washed with PBS and then immediately imaged by AFM in diH₂O.

The slides were imaged on an Asylum MFP-3D AFM scope (Santa Barbara, CA) using either a Nanoworld pyrex-nitride cantilever (Switzerland) or a Bruker SNL-10 #8 large cantilever (Camarillo, CA) in single point force curve map mode with sufficient resolution to distinguish the individual bacteria. Force curves were obtained by extracting the curves at points on the map corresponding to the highest elevation, which we took to be the apex of bacteria. For each curve, tip displacement was converted to force (F) by applying Hertz law $F = -kx$, where k is the spring constant of the cantilever tip as

measured in dH_2O , x is the displacement of the cantilever tip in meters, and F is force in Newtons.

Transmission electron microscopy

Negative staining transmission electron microscopy (TEM) was performed as previously described with some modifications (Kehl-Fie and St Geme 2007). Bacteria resuspended in 200 mM ammonium acetate were absorbed onto carbon/Formvar coated copper mesh grids for 1 minute and then washed once with dH_2O , with excess wash removed by gentle wicking. The grids were stained with uranyl acetate for 1 minute, with the excess stain wicked away and allowed to air dry. The grids were then examined by TEM using a JEOL 1010 electron microscope (Westmont, IL) fitted with a Hamamatsu digital camera (Japan) and AMT image capture software (Woburn, MA).

TEM with cationic ferritin staining of the capsule was performed as previously described (Starr, Porsch et al. 2016). Grids were examined using a JEOL 1010 electron microscope fitted with a Hamamatsu digital camera and AMT image capture software.

Western Blot

Western blot detection of Knh expression by strains KK01 and KK03 was performed using formic acid treated outer membrane preparations as described previously (Porsch, Kehl-Fie et al. 2012). In brief, starting with equal OD_{600} suspensions of bacteria, we

prepared outer membranes by sonication and sarkosyl solubility. Preparations were then formic acid treated to dissociate the Knh trimer, resolved on a 7.5% SDS-PAGE gel, and transferred to a nitrocellulose membrane. After blocking the membrane with 5% milk in PBS, Knh was detected using antiserum GP97, raised against the head region of Knh.

This chapter has been published in the Journal of Bacteriology with the following citation:

Kern, B. K., E. A. Porsch and J. W. St Geme, 3rd (2017). "Defining the Mechanical Determinants of *Kingella kingae* Adherence to Host Cells." *J Bacteriol* 199(23).

Strain	Background	T4P	T4P Retraction	Capsule	Knh	Source
WT	KK01	+	+	+	+	(Kehl-Fie and St Geme 2007)
KK01 <i>ctrA</i>	KK01	+	+	-	+	(Porsch, Kehl-Fie et al. 2012)*
KK01 <i>knh</i>	KK01	+	+	+	-	(Porsch, Kehl-Fie et al. 2012)*
KK01 <i>pilT</i>	KK01	+	-	+	+	(Porsch, Kehl-Fie et al. 2012)*
KK01 <i>pilA1ctrA</i>	KK01	-	NA	-	+	(Porsch, Kehl-Fie et al. 2012)*
KK01 <i>knhctrA</i>	KK01	+	+	-	-	(Porsch, Kehl-Fie et al. 2012)*
KK01 <i>pilA1knh</i>	KK01	-	NA	+	-	(Porsch, Kehl-Fie et al. 2012)*
KK01 <i>pilA1knhctrA</i>	KK01	-	NA	-	-	(Porsch, Kehl-Fie et al. 2012)*
KK03 <i>pilA1ctrA</i>	KK03	-	NA	-	+	(Porsch, Kehl-Fie et al. 2012)
KK03 <i>pilA1knhctrA</i>	KK03	-	NA	-	-	(Porsch, Kehl-Fie et al. 2012)

Table 1. Strain list. *Strains were made as described, but in the KK01 background.

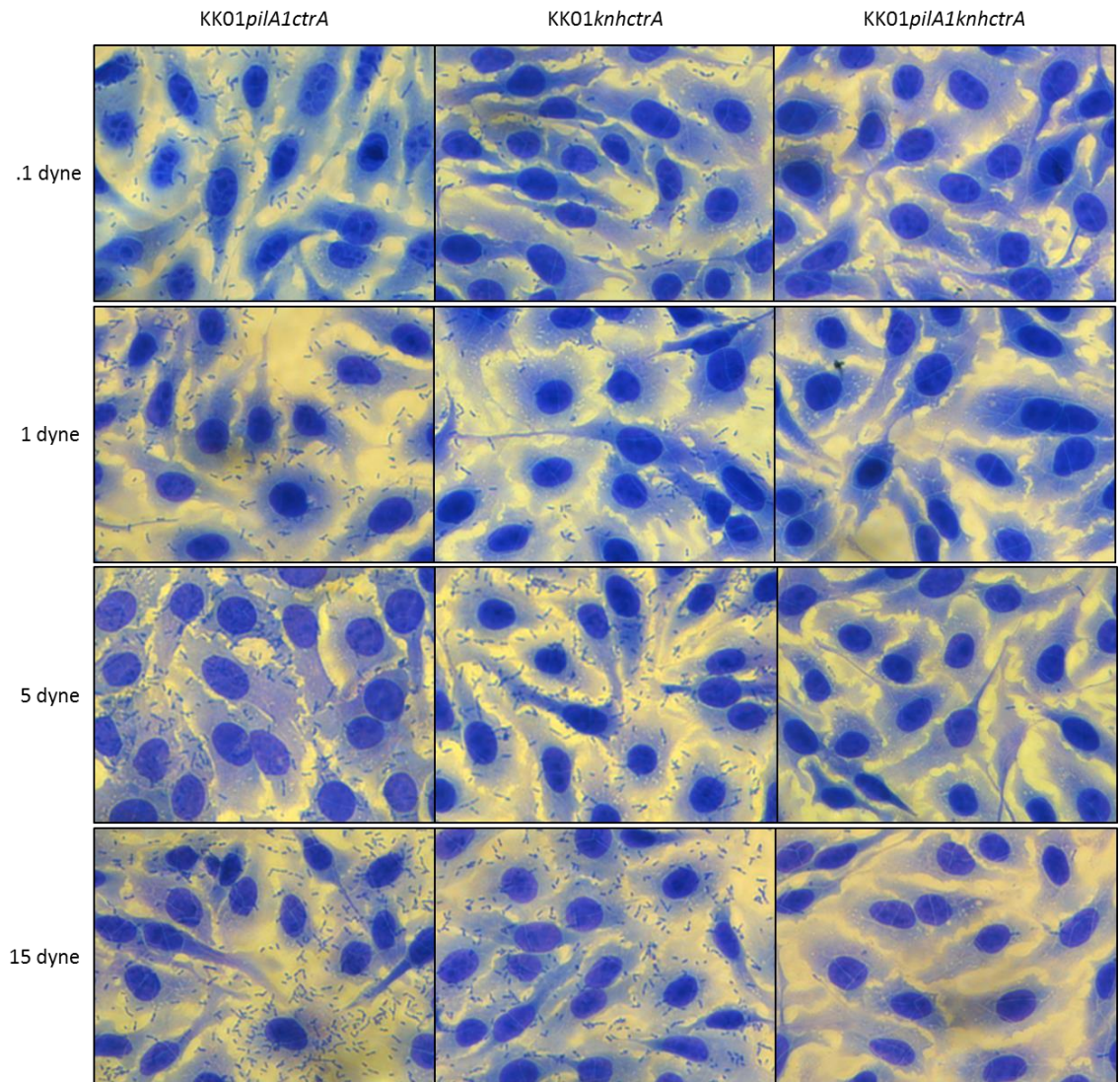


Figure S1. Representative frames from SRA assays.

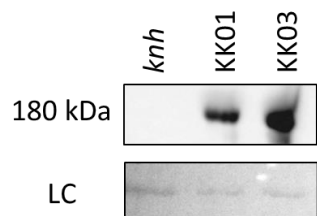


Figure S2. Western blot of *K. kingae* outer membrane preparations. Formic acid treated outer membrane preparations and Western blots were performed as described in Porsch 2012. The Knh monomer runs at approximately 170 kDa. Loading control (LC) is a ~70 kDa band visible by Ponceau S staining of the nitrocellulose membrane.

CHAPTER 3: Knh is a multifunctional adhesin produced by *Kingella kingae*

3.1 Introduction

Kingella kingae is a gram-negative bacterium that produces a trimeric autotransporter adhesin (TAA) called Knh. In previous work we demonstrated that Knh is a major adhesin responsible for tight-adherence to Chang cell monolayers (Porsch, Kehl-Fie et al. 2012, Kern, Porsch et al. 2017). TAAs are characterized by a C-terminal four β -sheet membrane anchor domain that trimerizes to form a twelve strand β -barrel pore in the outer membrane of the bacterium (Surana, Cutter et al. 2004). Insertion of the β -barrel into the outer membrane is known to be BamA dependent (Lehr, Schutz et al. 2010). The N-terminal passenger domain is translocated across the outer membrane and trimerizes to form a rod-like structure.

Although TAAs are a diverse family of molecules, structural motifs within the passenger domain are strongly conserved within the family. A common example is the β -roll structure of the globular head domain of YadA (YLHD) from *Yersinia enterocolitica*, conferring the signature lollipop shape to YadA when viewed by electron microscopy (EM). The YLHD has structural homologues in many TAAs from other species, including Knh (Porsch, Kehl-Fie et al. 2012). These structural homologues are frequently identified by amino acid sequence homology (Szczesny and Lupas 2008).

All TAAs characterized to date have been shown to have adhesive activity. Common targets include host cell membrane proteins, extracellular matrix (ECM) proteins, and soluble complement factors. There is a growing understanding of the structures that mediate the adhesive activities of TAAs. Two of the better studied examples are Hia/Hsf from *Haemophilus influenzae* and BadA from *Bartonella henselae*

In *H. influenzae*, Hia is produced by nontypeable (nonencapsulated) strains while Hsf is produced by encapsulated strains. Hia and Hsf are considered variants of each other, varying in length and number of binding domain (BD) motifs (Cotter, Surana et al. 2005). Hia has two BD motifs and Hsf has three BD motifs, in all cases characterized by a repeating motif of a TRP ring immediately followed by a C-terminal IS Neck motif (Laarmann, Cutter et al. 2002, Yeo, Cotter et al. 2004, Cotter, Surana et al. 2005). Interestingly, despite the evidence that BD1 and BD2 of Hsf mediate adherence to the same host cell receptor, only BD2 binds to vitronectin (Vn) (Singh, Su et al. 2014).

BadA is a very large TAA expressed by *B. henselae*. The head region and stalk regions of BadA have been shown to have overlapping as well as distinct adhesive properties, mediating adherence to ECM proteins (Kaiser, Linke et al. 2012). Specifically, the head region and stalk both mediate adherence to host cell monolayers and bind collagen, but only the stalk binds to fibronectin. Furthermore, only four out of the twenty-three stalk repeats are required for adherence to host cells. Hsf and BadA demonstrate how TAAs can be multi-functional adhesins.

Although TAA architecture is conserved across the family, binding partners and host cell receptors can vary widely. In this study we leverage part of our substantial collection of *K. kingae* clinical isolates to examine the sequence diversity of Knh. Additionally, we characterize the adhesive activity of Knh in assays with diverse cell lines and purified ECM proteins using our prototype strain KK01 and clinical isolates producing Knh variants.

3.2 Results

***K. kingae* clinical isolates from different clonal groups produce variant Knh molecules.** We examined formic acid treated outer membrane preparations from epidemiologically distinct clinical isolates of *K. kingae* by Western blot. As shown in Figure 1A, using antiserum GP97 against the YLHD of Knh01, we observed reactive bands that ranged in apparent molecular mass from ~150 kDa to ~190 kDa. When we compared the Knh from isolates within the same clonal group, we observed that the apparent molecular mass varied clonally (Figure 1B).

Knh variants are clonal. We sequenced 95 strains and were able to assemble 21 complete *knh* sequences, in addition to Knh01 from our prototype strain KK01 (Porsch, Kehl-Fie et al. 2012). These sequences originated from seven PFGE clonal groups, H, K, B, D, U, J, and S, and were grouped into six variants by homology. Knh variation was clonal, with sequences originating from within a clonal group having predicted amino

acid sequences with greater than 99% identity, except clonal groups J and S, which shared a Knh variant (data not shown).

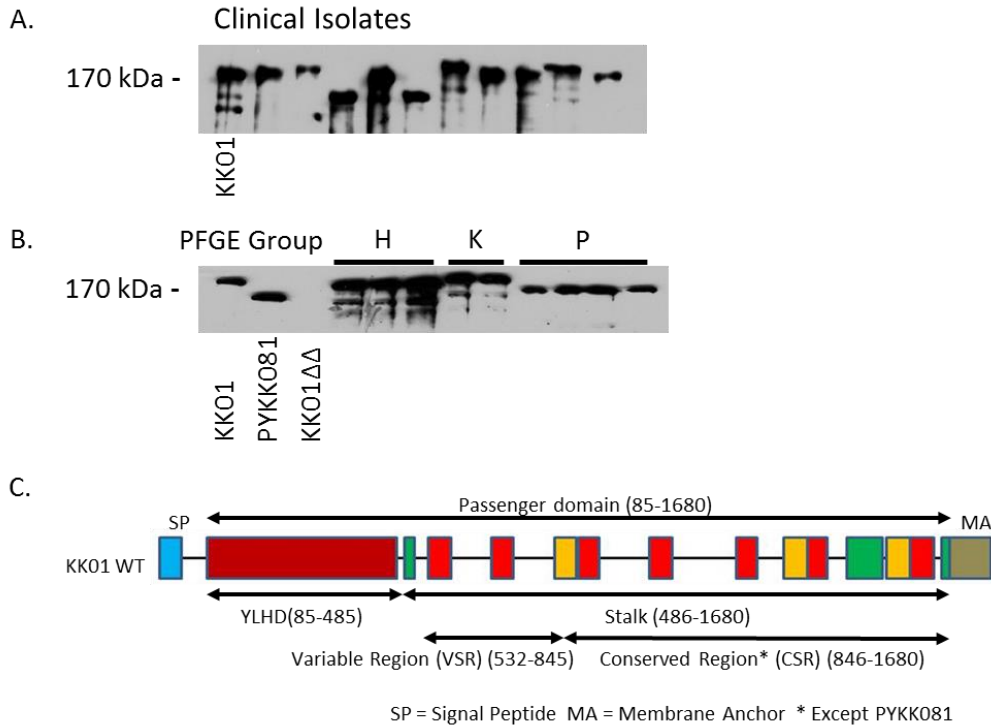


Figure 1. Knh variability among clinical isolates. A and B) Western blot analysis of formic acid treated outer membrane preparations from epidemiologically unrelated selection of clinical isolates. Knh variants were detected using antibody GP97 which detects the YLHD. C) Illustration of Knh highlighting the regions of Knh.

Sequence alignments revealed a variable region in Knh. Alignments of the predicted amino acid sequences of the Knh variants revealed regions within the passenger domain with substantial identity (Figure 1C). These highly conserved regions corresponded to residues 1-531 and 846-1783 in our prototype Knh from strain KK01 and included the

predicted signal peptide, YLHD, C-terminal of the stalk domain, and membrane anchor. The N-terminal region of the stalk region was the most variable, with variations in both sequence and length. We have named this region of the stalk domain the variable stalk region (VSR) and the highly conserved C-terminal region the conserved stalk region (CSR). The signal peptide and membrane anchor had greater than 95% amino acid sequence identity across all variants. The YLHD had approximately 80% amino acid identity across the variants, while the CSR had approximately 90% amino acid identity across all variants with the exception of Knh081. The VSR contained approximately 40% identity across the variants. Knh081 had a 193 residue insertion in the CSR between the amino acids corresponding to 1472 and 1473 of Knh01. Knh081 was also significantly shorter than the other variants due to significant deletions in the VSR.

Knh variants mediated adherence to host cells. We tested the adherence of representative clinical isolates to host cell monolayers using our standard adherence assay. In order to isolate the adherence activities of Knh, we made *pilA1* and capsule synthesis double mutant strains, denoted as $\Delta\Delta$, in each clinical isolate. Elimination of the major pilin subunit *pilA1* gene results in a nonpiliated strain. Elimination of the capsule synthesis locus results in a nonencapsulated strain. Elimination of the capsule and T4P major pilin did not change the expression of Knh (data not shown). We were able to find transformable strains in only four of the five clonal groups, and we therefore proceeded with our prototype strain KK01 and four clinical isolates: PYKK060, PYKK081, PYKK086, and PYBB270. Negative control strains were made by further eliminating the *knh* gene, thus Knh expression, and these strains are denoted as $\Delta\Delta\Delta$.

As shown in Figure 2, all *Knh* variants mediated adherence to Chang cells. *KK01ΔΔ*, *KK060ΔΔ*, *KK081ΔΔ*, and *KK086ΔΔ* were capable of adherence to Chang cells at ~40-50% of inoculum. *BB270ΔΔ* demonstrated much lower adherence to Chang cells at 14% of inoculum. Adherence to A549 cells was much more variable, with a range between 2.8% (*BB270ΔΔ*) and 53.4% (*KK081ΔΔ*). Adherence by all $\Delta\Delta$ strains to both Chang cells and A549 cells was significantly higher than the corresponding $\Delta\Delta\Delta$ negative control strains ($p < .05$).

The YLHD and stalk of *Knh01* mediated adherence to Chang cells. To test the ability of the YLHD and the stalk region to mediate adherence to Chang cells, we produced strains that expressed shortened versions of *Knh01*. As shown in Figure 3A, the *Knh01YO* passenger domain was comprised of only the YLHD and was produced by strain *KK01YO*. Conversely the *Knh01NY* passenger domain was comprised of only the stalk region and was produced by *KK01NY*. We observed that a strain producing either construct had significantly higher adherence to Chang cells than the *KK01 knh* strain ($p < .05$) (Figure 3B and C). A *KK01 pilA1* mutant strain, deficient for T4P production, was included as a negative control.

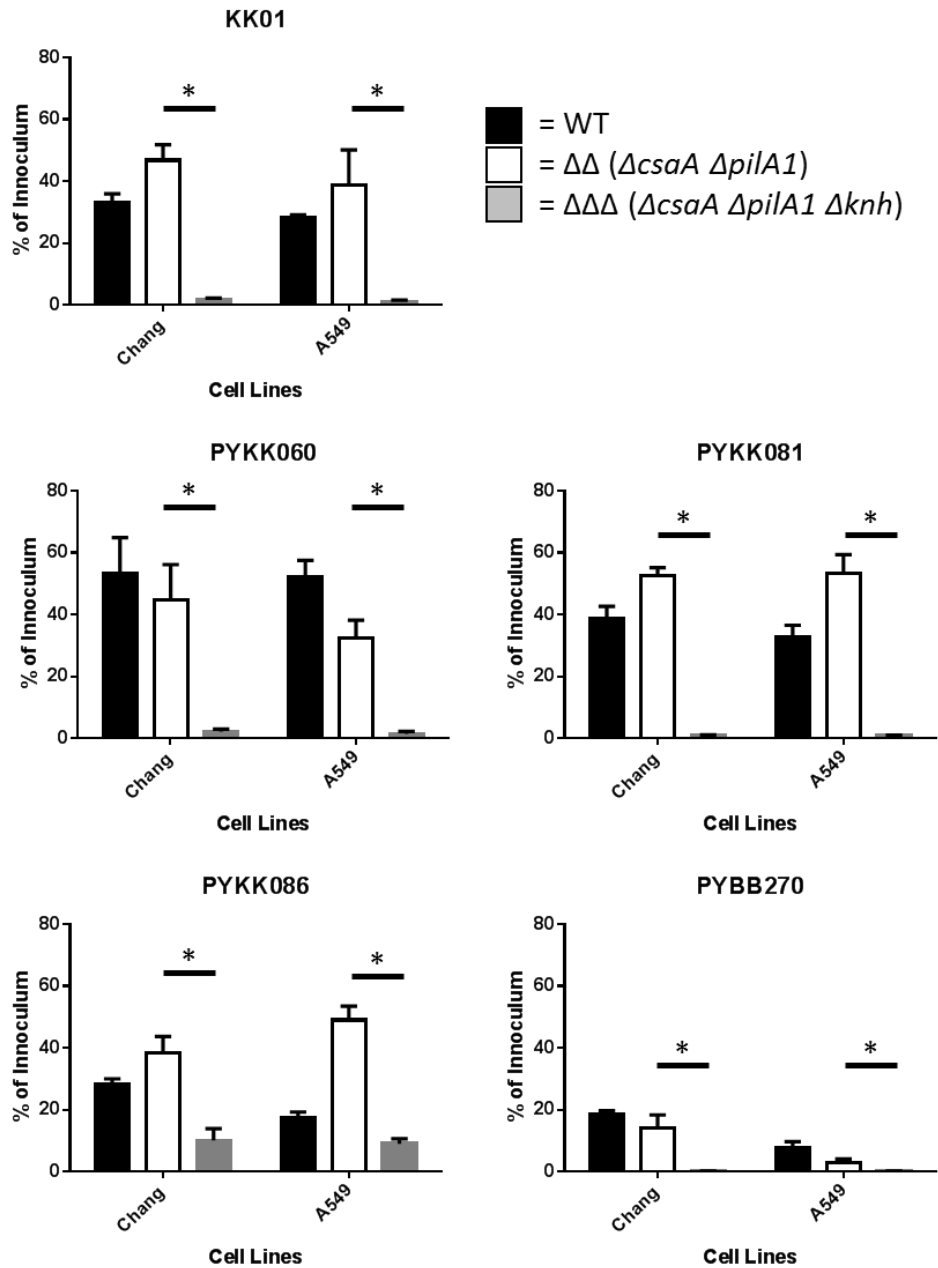


Figure 2. Knh variant adherence to host cells. Mutant strains deficient in T4P and capsule (white bars) were tested for their adherence to Chang cell and A549 cell monolayers using our standard adherence assay. The T4P, capsule, and Knh triple mutants (gray bars) and wild type strains (black bars) are included for comparison. * $p < 0.05$

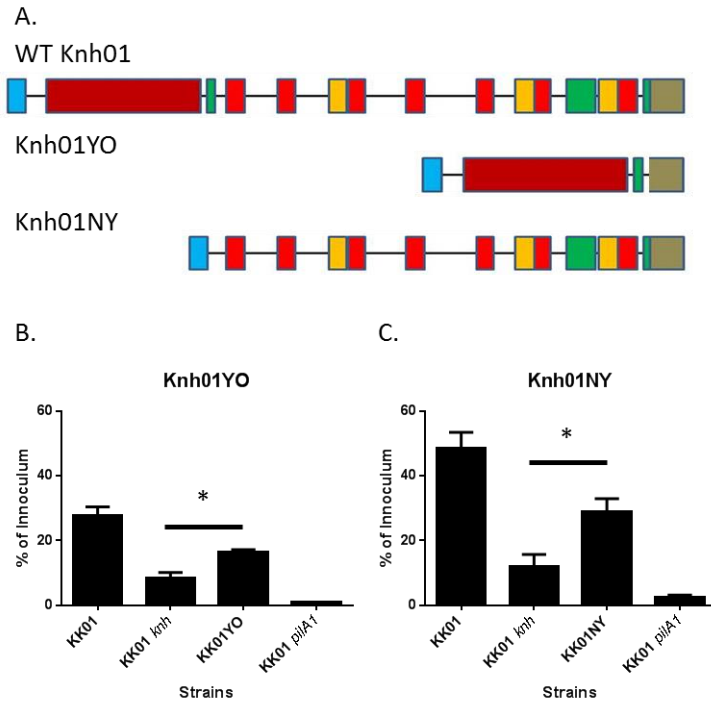


Figure 3. YLHD and stalk region adherence to Chang cells. A) Illustration of Knh variants with either the stalk (Knh01YO) or YLHD (Knh01NY) deleted. Standard adherence assays were performed to examine the adherence of KK01 strains producing Knh variants B) Knh01YO and C) Knh01NY to Chang cells. Adherence is compared to a KK01 *knh* strain. * $p < 0.05$

Knh variants mediated adherence to ECM protein coated plates. We sought to determine whether the Knh variants produced by clinical isolates were capable of mediating adherence to ECM proteins (Figure 4). Using plates coated with recombinant human vitronectin (rhVn), fibronectin, laminin, collagen I, or collagen IV, we observed generally lower adherence to ECM protein coated plates than host cells; however, our results showed that Knh mediated substantial adherence to specific ECM proteins. The pattern of adherence was not consistent across the clinical isolates. All clinical isolate $\Delta\Delta$ derivatives except KK086 $\Delta\Delta$ demonstrated substantial adherence to rhVn at levels

similar to those of their parent strains. Our prototype strain KK01 $\Delta\Delta$ demonstrated adherence to rhVn, but no other ECM proteins. Other variants demonstrated adherence to other ECM proteins. KK060 $\Delta\Delta$ was the only strain capable of significant adherence to laminin. Strains KK081 $\Delta\Delta$ and BB270 $\Delta\Delta$ were capable of significant adherence to collagen IV. None of the triple mutant negative control strains displayed any detectable adherence to any of the coated plates.

The head and stalk of Knh01 mediated adherence to Vn. Using our standard static adherence assay as modified for ECM protein coated plates, we observed that derivatives that produced Knh variants Knh01YO and Knh01NY were capable of adherence to rhVn coated plates (Figure 5A). We observed adherence to Vn coated plates of 15.4% for the KK01NY $\Delta\Delta$ strain and 10.4% for the KK01YO $\Delta\Delta$ strain. Adherence by the KK01 $\Delta\Delta\Delta$ mutant strain was below the limit of detection.

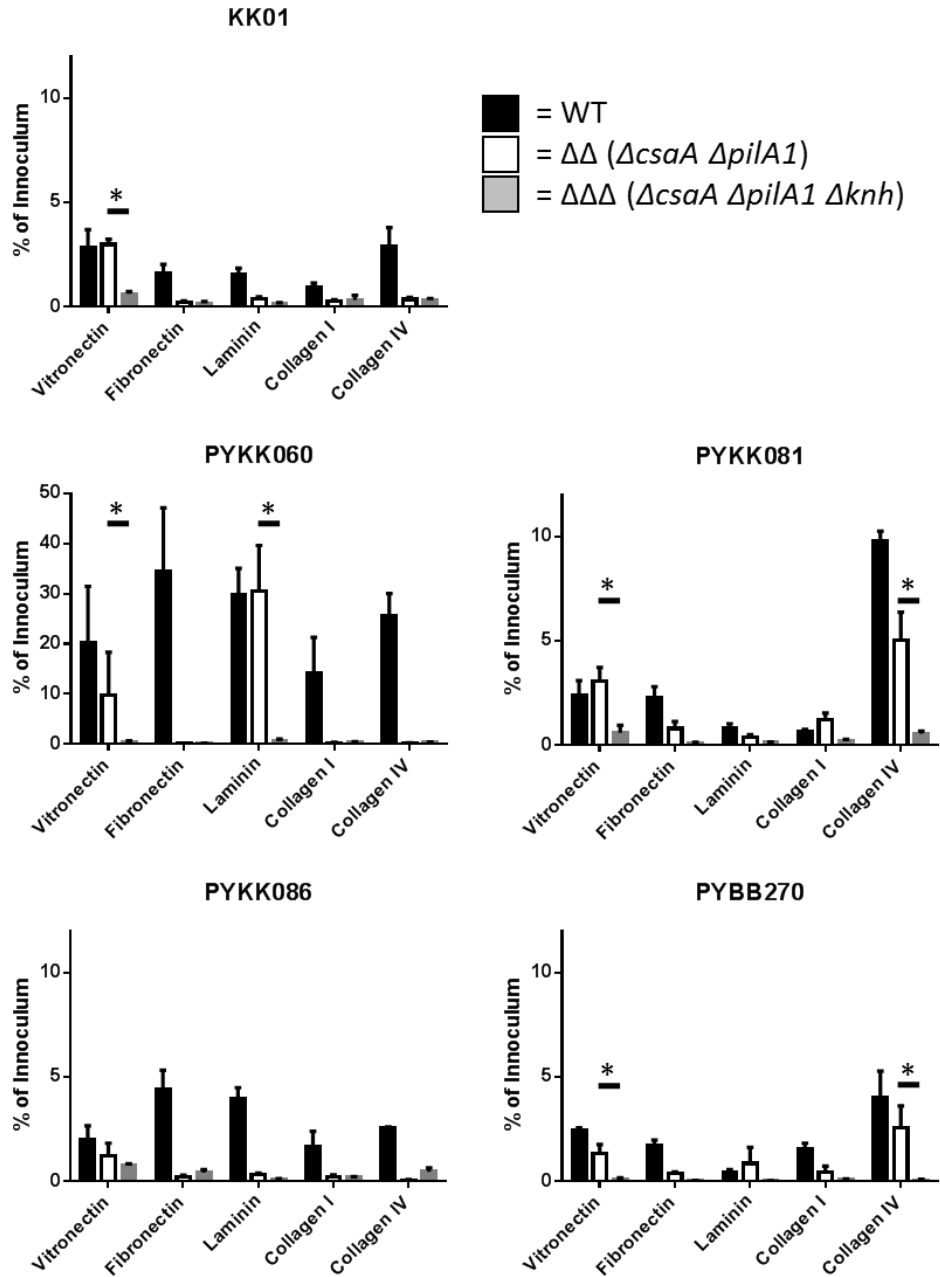


Figure 4. Knh variant adherence to ECM proteins. Mutant strains deficient in T4P and capsule (white bars) were tested for their adherence to vitronectin, fibronectin, laminin, collagen I, collagen IV coated plates using a modified standard adherence assay. The T4P, capsule, and Knh triple mutants (gray bars) and wild type strains (black bars) are included for comparison. * $p < 0.05$

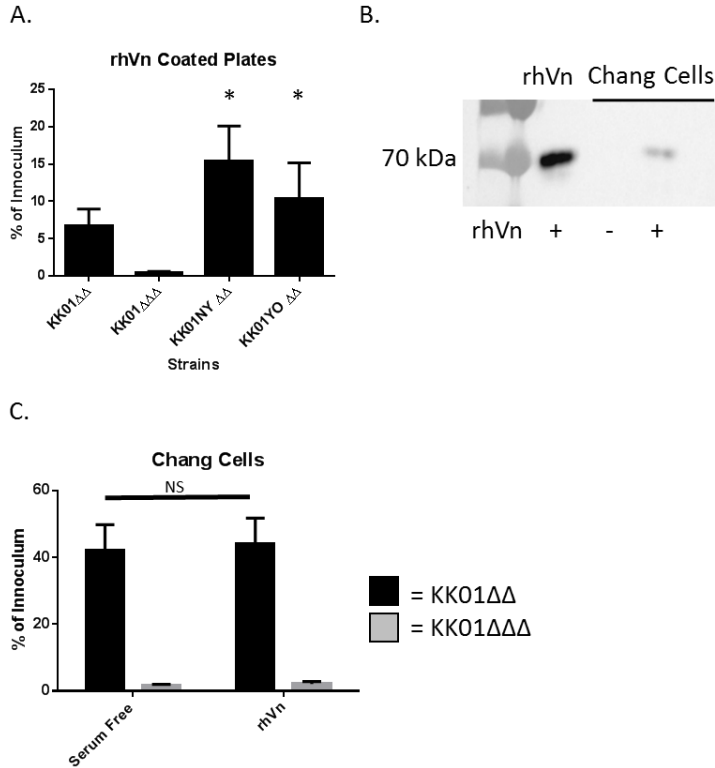


Figure 5. Knh YLHD and stalk region adhering to rhVN. A) KK01 strains expressing Knh01YO and Knh01NY demonstrate adherence to rhVn coated plates. Strains used were $\Delta csaA \Delta pilA1$ ($\Delta\Delta$) or $\Delta csaA \Delta pilA1 \Delta knh$ ($\Delta\Delta\Delta$). * $p < 0.05$ B) Chang cells maintained in serum-free conditions can acquire rhVn from the media. rhVn detected by Western blot. C) Strain KK01 $\Delta\Delta$ (black bars) is able to adhere to Chang cell monolayers incubated in serum-free media supplemented with 5ug/ml rhVn and Chang cell monolayers maintained in serum-free media. KK01 $\Delta\Delta\Delta$ (gray bars) included as a negative control.

Chang cell monolayers acquired environmental Vn. Whole cell lysates of Chang cell monolayers incubated for 2 hours in serum-free medium supplemented with rhVn prior to harvest contained detectable Vn by Western blot (Figure 5C). Chang cell monolayers maintained in serum-free conditions did not contain any detectable Vn by Western

analysis. We tested whether Vn binding by Chang cells enhanced adherence by Knh-producing *K. kingae*. We compared the adherence of KK01 $\Delta\Delta$ to Chang cell monolayers maintained in serum-free medium versus KK01 $\Delta\Delta$ adherence to Chang cell monolayers maintained in rhVn-supplemented serum-free medium. There was no observable difference in Knh-mediated adherence between monolayers kept serum-free and monolayers supplemented with rhVn (Figure 5D).

3.3 Discussion

In this study we examined the predicted amino acid sequences of the Knh variants produced by clinical isolates and observed that they have significant variation between them, attributable primarily to the variable N-terminal region of the stalk. Examination of select Knh variants for adherence to host cells and ECM proteins revealed that all variants mediated adherence to Chang and A549 cells. Four of the five variants mediated significant adherence to Vn, and several variants were found to adhere to collagen IV or laminin as well. We used our prototype Knh variant to determine that both the YLHD and stalk regions of the passenger domain could bind Vn and that this binding does not contribute to adherence to Chang cells, suggesting that Chang cell express a separate receptor for Knh. These data suggest that Knh is a multifunctional adhesin and demonstrate that Knh variants produced by clinical isolates have differential adhesive activity.

Western blot detection of Knh variants produced by clinical isolates suggests that there is likely an even greater diversity of Knh variants than we were able to examine in this work. Alignments of the predicted amino acid sequences of Knh produced by clinical isolates showed that Knh varied clonally, except clonal groups J and S, which share a Knh variant. The pattern of variation was striking, although we were only able to examine a limited set of variants. We observed regions of identity that include the signal peptide, the YLHD, the C-terminal portion of the stalk (CSR), and the C-terminal translocation domain. In contrast, the N-terminal portion of the stalk (VSR) had maximal variation.

We hypothesized that Knh variants might have differential adherence activities, and we examined the adhesive activities associated with the Knh variants to host cells and ECM proteins. All five Knh variants we examined were able to mediate adherence to both Chang cells and A549 cells, consistent with our hypothesis that Knh-mediated adherence plays a role in colonization of the respiratory tract. Adherence to cell lines could be a starting point for determining potential host receptors, though it is not necessarily indicative of *in vivo* TAA performance. Further work will be needed to determine the actual receptor molecules expressed by Chang cells and A549 cells.

To begin to localize the adherence to Chang cells to Knh domains, we created constructs that produced Knh variants lacking either the entire stalk (Knh01YO) or the YLHD (Knh01NY). We tested these constructs for their adherence to Chang cells using

our standard adherence assay and found that both mediated adherence significantly above that of a Knh deficient strain. Interestingly, adherence by both constructs was T4P dependent and elimination of T4P, even in a nonencapsulated background, resulted in abrogation of adherence by these constructs. This suggests that these constructs are too short to mediate adherence independently of T4P. In the case of Knh01NY, it is possible that adherence to Chang cells is localized to the C-terminal portion of the stalk. This could have the effect of making stalk-mediated adherence to Chang cells T4P dependent, even if the stalk as a whole is long enough to make contact with the host cell.

Our work also demonstrated that Knh is capable of mediating adherence to ECM proteins. It is noteworthy that there were significant differences among Knh variants in adherence to ECM proteins. Four of the five Knh variants adhered to rhVn. The Knh variant from PYKK060 adhered to laminin as well, and the Knh variants from PYKK081 and PYBB270 adhered to collagen IV as well. These results are interesting, as both laminin and collagen IV are found in the basal lamina of epithelial membranes. Given the ubiquitous nature of these ECM proteins in epithelial layers, it is surprising that only a portion of the Knh variants had observable adherence to them. On the other hand, it is possible that the basal lamina would only be available to Knh binding if the overlying epithelial layer were breached. A breach in the epithelium could be caused by a viral coinfection or by the potent RTX toxin produced by *K. kingae* (Kehl-Fie and St Geme 2007). It therefore could be hypothesized that strains producing Knh variants that

adhere to laminin or collagen IV are more likely to be associated with invasive disease and this possibility warrants further investigation.

The binding to Vn by four out of the five Knh variants suggests a role for Knh-mediated Vn binding in the lifestyle of *K. kingae*. Vn is a soluble glycoprotein that is found in serum and the extracellular matrix. It is the ligand for the $\alpha V\beta 3$ integrin and inhibits complement pathways (Dahlback and Podack 1985, Horton 1997). Binding of Vn by Hsf contributes to *H. influenzae* adherence to A549 cells and to serum resistance (Hallstrom, Trajkovska et al. 2006, Singh, Su et al. 2014). Using our prototype strain we further investigated Knh binding to Vn. We observed that both the YLHD and stalk of Knh mediated adherence to rhVn coated plates, providing evidence that the YLHD mediates Vn binding, and that the stalk also contains one or more domains that bind Vn. Strain KK01 $\Delta\Delta$ had the same level of adherence to Chang cells in serum-free medium and to Chang cells supplemented with purified rhVn despite evidence that both Chang cells and bacteria expressing Knh can bind Vn. This observation suggests that there is a separate receptor on Chang cells that binds Knh to mediate the high level of adherence we observe. It is possible that Vn binding may play a role in Knh-mediated adherence to other cell lines and this will need to be determined on a line-by-line basis. Taken together, these data suggest that Knh is a multi-purpose adhesin and that variation of Knh among clinical isolates leads to diverse adhesive activities.

One important caveat related our adherence assays is that we were unable to express the Knh variants in a common background due to the Knh passenger domain being AT-rich, making cloning in that region difficult. We instead created mutants deficient in capsule and T4P in clinical isolates that produced a Knh variant of interest. Therefore, we could not control for levels of Knh expression strain-to-strain, limiting our inter-strain comparisons of Knh-mediated adherence. However, when we compare KK01 to its highly piliated variant KK03 (Kehl-Fie, Miller et al. 2008), which also expresses a much higher level of Knh (Kern, Porsch et al. 2017), we see no difference in Knh-mediated adherence to respiratory cells or Vn coated plates using our standard adherence assay (data not shown). This observation suggests that the amount of Knh produced by a strain does not affect the level of Knh-mediated adherence.

The variation within the VSR could potentially lead to a diverse repertoire of Knh receptors. Even with our limited set of ECM proteins, we observed significant differences in adhesive activity between Knh variants. One could hypothesize that these differences in adhesive activity between Knh variants will be localized to the VSR. One could also hypothesize that activities that are common to all of the variants, such as adherence to Chang cells and A549 cells, will be localized to the CSR. We attempted to make variants of Knh that expressed either the VSR or CSR only in our prototype strain KK01; however, again due to the AT-richness of the passenger domain, cloning those fragments proved difficult to do in a timely manner. Future experiments will be needed to determine the contribution of the VSR and CSR to the adhesive activities of the stalk domain.

Intraspecies genetic variation in TAAs has been well studied in some instances, including VtaA from *Haemophilus parasuis* (Pina, Olvera et al. 2009) and the group I and group II NadA adhesins from *Neisseria meningitidis* (Comanducci, Bambini et al. 2004, Bambini, De Chiara et al. 2014). Here we examined the diversity of Knh molecules produced by a selection of *K. kingae* clinical isolates and determined their adherence activities to epithelial cells and ECM proteins. The work presented here is the first description that Knh is a multifunctional adhesin and that variation of Knh among *K. kingae* clinical isolates is associated with diverse adhesive activities.

3.4 Materials and Methods

Strains and constructs

Strains used are summarized in Table 1. *K. kingae* strains were grown at 37°C and 5% CO₂ on chocolate II agar plates from frozen stocks for 17-18 hours prior to use in assays. Clinical isolates were obtained from Pablo Yagupsky from Soroka University Medical Center, Israel. Mutant *K. kingae* strains were generated from the clinical isolates as described previously using either plasmid DNA or genomic DNA containing the desired mutation and an antibiotic resistance cassette (Porsch, Kehl-Fie et al. 2012, Starr, Porsch et al. 2016).

Knh truncations were created in our prototype strain KK01 via allelic exchange using overlap PCR products as follows. Overlap PCR precursor products were made using the primers listed in Table 2. Matching upstream and downstream precursor products

were then used as templates in a PCR reaction with the appropriate complementing forward and reverse primers to produce the full length overlap PCR product.

Full length overlap PCR products were transformed into strain KK01 using a spot transformation protocol. Briefly, bacteria were resuspended from overnight culture plates to an OD₆₀₀ of 0.8. This suspension was diluted 1:100 and then serially diluted 1:4 for a total of 9 dilutions. Five µl of the 5 lowest dilutions was mixed with 5 µl of overlap PCR product at 100-200 µg/µl. All 10 µl of the transformation mixture was plated on chocolate II agar plates (BD). The transformation plates were grown overnight, and single colonies were picked. Genomic DNA was extracted and PCR screened using the KnhF1 and Knh R1 primers, and colonies with the correct sized PCR product were subjected to Sanger sequencing to confirm the truncation. The resulting KK01 strains expressed Knh passenger domains with either the YLHD only (KnhYO) or the stalk only (KnhNY) (Figure 4A).

Cultured cell lines

Cell lines were maintained at 37°C and 5% CO₂. Chang cells were grown in MEM media supplemented with 10% FBS and 1% non-essential amino acids. A549 cells were grown in MEM media supplemented with 10% FBS. Cells lines were cultured from frozen stock and split as necessary.

Sequencing *K. kingae* clinical isolates

Genomic DNA from clinical isolates was prepared using the Wizard Genomic DNA purification kit (Promega) as directed for gram-negative bacteria. Genomes were then fragmented and barcoded using the Nextera XT kit (Illumina) and sequenced on an Illumina HiSeq 2500 machine using a 100SR single end read protocol.

Single nucleotide polymorphisms calling and phylogenetic matrix construction

Comparison of single nucleotide polymorphisms (SNP) between isolates was done using short read alignment to the genome of *K. kingae* strain KWG1 (Bidet, Basmaci et al. 2016) as reference using the Burrows-Wheeler Alignment (bwa) tool (<http://bio-bwa.sourceforge.net>). SNP calls were made using samtools (<http://samtools.sourceforge.net>). SNPs were identified as “high quality” if they were not listed as “heterozygous” and had a per base Q score greater than or equal to 20. For preassembled genomes from public databases, we used whole-genome alignment with reference to the KWG1 genome using the show-snps utility of NUCmer (<http://mummer.sourceforge.net>). All regions from the reference genome annotated as mobile genetic elements were excluded. We also applied a mask that excluded repetitive sequences from the reference genome that were more than 80% identical over at least 100 nucleotides to other genomic loci using a pairwise MegaBLAST-based analysis.

Phylogenetic Analyses

Maximum likelihood (ML) phylogenies were constructed with the POSIX-threads RAxML v8.0.19 (Stamatakis 2006). We used an ascertainment bias correction and a general time-reversible (GTR) substitution model (Lanave, Preparata et al. 1984) accounting for among-site rate heterogeneity using the Γ distribution and four rate categories (Yang 1994) (ASC_GTRGAMMA model) for 100 individual searches with maximum parsimony random-addition starting trees. Node support was evaluated with 1000 nonparametric bootstrap pseudoreplicates (Felsenstein 1985). The number of bootstrap pseudoreplicates over which node support is not expected to be significantly altered was evaluated using the frequency-based (300 bootstrap iterations were sufficient) and extended majority-rule (550 bootstrap iterations were sufficient) bootstrapping criteria (Pattengale, Alipour et al. 2010).

Alignments

Alignments of multiple *knh* nucleotide sequences were performed using MAFT under the default parameters (Katoh, Rozewicki et al. 2017). Amino acid sequence alignments were performed using Clustal Omega under the default parameters (Sievers, Wilm et al. 2011).

Outer membrane preparations to detect Knh

Outer membrane preparations based on sarkosyl insolubility were performed as described previously (Porsch, Kehl-Fie et al. 2012). Preparations were resolved on 7.5% SDS PAGE gels, transferred to nitrocellulose membranes, and blocked using 5% milk in PBS. Knh was detected using either antiserum GP97 or antiserum CHOP-GP13 directed against Knh. GP97 was raised against a purified fragment of the YLHD as described in Porsch et al. (2012), and CHOP-GP13 was raised against a purified fragment from the conserved region of the stalk (aa 1192-1694) in the same manner as GP97.

Coomassie blue gel to detect PilA1

Pili preparations were performed as previously described (Kehl-Fie, Porsch et al. 2009). Preparations were resolved on 15% SDS PAGE gels and stained with Coomassie blue for 30 minutes. Gels were destained and imaged.

Adherence assays to host cell monolayers

Adherence assays were performed to fixed host cell monolayers in 24-well plates as previously described (Kehl-Fie, Miller et al. 2008). Bacteria were resuspended in PBS to an OD₆₀₀ of 0.8, giving a consistent inoculum with all strains. An inoculum of approximately 4.0×10^6 was added to each well, and plates were centrifuged at 165 x g for 5 minutes to settle the bacteria onto the cell monolayers. The plates were then

incubated for 25 minutes at 37°C. Non-adherent bacteria were washed away with three washes of PBS, and 100 µl of 0.05% trypsin-EDTA (Sigma) was then added to each infected well to release adherent bacteria. Serial dilutions of the resuspended bacteria were plated for CFUs. All experiments were performed in triplicate. Results are reported as a percentage of the inoculum, and significance was determined by the Student t-test.

Adherence assays to ECM protein coated plates

We slightly modified our standard adherence assay to host cell monolayers to be used with ECM protein coated plates. Bacterial adherence to collagen I, collagen IV, fibronectin, and laminin pre-coated plates (BD) was tested. We also coated plates with purified recombinant human vitronectin (rhVn) as follows. 300 µl of purified truncated recombinant human vitronectin (Thermo Fisher) at 5 µg/ml in PBS was added to each well of a 24-well tissue culture plate and incubated at 4°C for 17-18 hours. Coated plates were washed with PBS once prior to being used in adherence assays.

300 µl of PBS was added to ECM protein coated plates in preparation for the adherence assay. Bacteria were resuspended in PBS to an OD₆₀₀ of 0.8, and an inoculum of approximately 4.0×10^6 was added to each well of the plates. The plates were centrifuged at 165 x g for 5 minutes to settle the bacteria onto the plate surface. The plates were then incubated for 25 minutes at 37°C. Non-adherent bacteria were washed away with three washes of PBS, and 300 µl of 0.05% trypsin-EDTA (Sigma) was added

to each infected well to release the adherent bacteria. Serial dilutions of the resuspended bacteria were plated for CFUs. Experiments were performed in triplicate. Results are reported as a percentage of the inoculum, and significance was determined by the Student t-test.

Chang cell monolayer binding of Vn

Chang cells were seeded into a tissue culture flask in serum-free media at a density that yielded confluent monolayers overnight. The monolayers were incubated for 17-18 hours overnight, and the media in the wells was replaced by serum-free MEM media supplemented with 5 µg/ml rhVn. After an additional 2 hour incubation at 37°C, the monolayers were washed with PBS and harvested by scraping. The cells were then lysed by sonication for three pulses of 30 seconds at 25% power on a Qsonica Sonicator Ultrasonic Processor (part no. Q500, Newtown, CT.). Sonicates were resolved on a 7.5% SDS-PAGE gel and transferred to nitrocellulose, and rhVn was detected using anti-Vn antibody NBP 2-52586 (Novus, Littleton, CO).

Vitronectin enhanced adherence assay

To determine whether Vn binding by Chang cells contributes to Knh-mediated adherence to Chang cell monolayers, we prepared our cell monolayers as follows. Cells were resuspended in serum-free media and seeded into 24-well cell culture plates at a density that resulted in a confluent monolayer overnight. Two hours prior to the assay,

the serum-free media was replaced with 300 µl of serum-free media supplemented with 5 µg/ml of rhVn. After a two hour incubation at 37°C, the monolayers were fixed and used in a standard adherence assay as summarized previously.

Strain	Capsule	T4P	Knh Variant	Clonal Group	Source
KK01	+	+	Knh01	H	Kehl-Fie 2008
KK01ΔΔ	-	-	Knh01		Starr 2016
KK01ΔΔΔ	-	-	-		This work
KK01 <i>knh</i>	+	+	-		Porsch 2012
KK01 <i>pilA1</i>	+	-	Knh01		Starr 2016
KK01YO	+	+	Knh01YO		This work ⁺
KK01YOΔΔ	-	-	Knh01YO		This work [*]
KK01NY	+	+	Knh01NY		This work ⁺
KK01NYΔΔ	-	-	Knh01NY		This work [*]
PYKK060	+	+	Knh060	D	P. Yagupsky
KK060ΔΔ	-	-	Knh060		This work [*]
KK060ΔΔΔ	-	-	-		This work [*]
PYKK081	+	+	Knh081	B	P. Yagupsky
KK081ΔΔ	-	-	Knh081		This work [*]
KK081ΔΔΔ	-	-	-		This work [*]
PYKK086	+	+	Knh086	K	P. Yagupsky
KK086ΔΔ	-	-	Knh086		This work [*]
KK086ΔΔΔ	-	-	-		This work [*]
PYKKBB270	+	+	Knh270	U	P. Yagupsky
BB270ΔΔ	-	-	Knh270		This work [*]
BB270ΔΔΔ	-	-	-		This work [*]

Table 1. Strains list. * = Strains produced as in Porsch et al. 2012 or Starr et al. 2016 except in the strain indicated. + = Strains produced via allelic exchange using overlap PCR products.

Primer	Sequence	Compliment Primer	Precursor product
KnhF1	GCATA TTGACGCGATTCAAGCC		
KnhR1	GCA TGGCAAGCTGCTCTCAAAGAATG		
Knh F6	GAGACCACA TTGCCGACTGG		
Knh R5	GATGCGATTGCTCCAAACGC		
KnhMCS R2*	gcgccgcAGCACCTGCGCCtggcgcgccATTGGTATTGACAGTACTATTTGGGCC	Knh F1	YO upstream
KnhMCS F2*	ggcgcgccGGCGCAGGTGCTgcgccgcccaattgtGCTGGCAACACGACTGTGAAG	Knh R5	YO downstream
KnhMCS R3*	gcgccgcAGCACCTGCGCCtggcgcgccCTGCGCCGTTAAAGGCAC	Knh F6	NY upstream
KnhMCS F3*	ggcgcgccGGCGCAGGTGCTgcgccgcccaattgtGCAAATAGTACTGCAACAAGCGTTG	Knh R1	NY downstream

Table 2. Primers used to produce overlap PCR products for deletion of Knh passenger domain regions.

CHAPTER 4 Summary and Future Directions

4.1 Summary

The work presented in chapters 2 and 3 sought to examine several aspects of TAA biology: how the spatial relationship of TAAs to other surface factors produced by a bacterium can affect TAA-mediated adherence and how sequence diversity in TAAs can lead to diverse adhesive activities. We found that our model of *K. kingae* adherence was essentially correct. We observed that Knh mediates adherence more resistant to shear forces than do T4P and that capsule is deeper than maximal Knh projection from the surface. We also observed that T4P retraction was necessary for Knh-mediated adherence, even under shear stress. We then examined the adhesive activity of Knh, in particular including its variation among clinical isolates and the variability of Knh-mediated adherence to host cells and ECM proteins. We demonstrated that all Knh variants mediated adherence to respiratory epithelial cells; however, we observed significant variation in adherence to ECM proteins.

4.2 Define the host receptor(s) of Knh

TAAs have been shown to have diverse host receptors. The work presented in chapter 3 examined a limited set of ECM components in addition to host cells. We also observed that Vn binding by strain KK01 did not enhance adherence to Chang cells, suggesting that Vn is not the receptor on Chang cells. Although ECM proteins are ubiquitous, they make up only one class of potential host receptors for Knh. TAAs have

been shown to target a variety of host surface proteins and soluble complement proteins, in addition to ECM components. However, the particular receptor remains unknown for many TAAs.

Additionally, TAAs can have multiple binding partners, conferring multifunctionality. Several prominent examples of TAAs bind multiple factors, for example fibronectin and collagen in the case of BadA (Kaiser, Linke et al. 2012) and collagen IV and tumor necrosis factor receptor 1 (TNFR-1) in the case of BcaA (El-Kirat-Chatel, Mil-Homens et al. 2013, Mil-Homens, Pinto et al. 2017). In the case of BcaA, collagen IV binding is thought to play a role in host colonization (El-Kirat-Chatel, Mil-Homens et al. 2013) and TNFR-1 binding promotes adherence to endothelial cells, but also promotes inflammation (Mil-Homens, Pinto et al. 2017). These examples demonstrate the multifunctionality of TAAs, though the physiological relevance of such multi-functionality is understood in only a few cases. Defining the host receptor(s) of Knh could advance our knowledge of *K. kingae* pathogenesis and TAA multifunctionality generally.

Knh is potentially an important factor for adherence in several physiological niches. Defining the host cell receptor(s) for Knh has the potential to lead to a better understanding of *K. kingae* pathogenesis. Host receptor specificity could potentially explain the apparent *K. kingae* tropism for bones and joints. It is possible that Knh specificity to receptors expressed by synovial cells and bone cells leads to *K. kingae* preferentially causing osteoarticular invasive disease. It is also possible that certain cell

types lack Knh receptors. For example, it would be reasonable to hypothesize that Knh does not mediate tight adherence to endothelial cells, thus allowing the bacterium to circulate through the vascular system and reach sites of invasive disease. Future experiments examining the role of Knh in colonization and pathogenesis will need to keep in mind that clinical isolates produce Knh variants which likely have corresponding variation in host cell receptor(s). This variability in receptor(s) can potentially alter the role of Knh in the context of colonization and disease.

4.3 Determine the relationship of Knh structure, flexibility and adhesive activity

Given the modularity of Knh, it would be interesting to map specific adhesive activities to specific regions or domains of the passenger domain. We have shown that Vn binding activity is localized to both the YLHD and stalk of our prototype Knh from strain KK01. Adhesive activity to the host cell has yet to be localized to a particular domain of the passenger domain. Additionally, we have delineated a conserved region (CSR) and variable region (VSR) of the stalk, and additional work will be needed to address the contribution of both of these regions to Knh-mediated adherence to both cell receptors and ECM proteins. Crystallization studies of the Knh passenger domain will be useful in confirming the predicted structure of the various domains and regions.

A relatively nascent field of study related to the structure of TAAs is the study of passenger domain flexibility. Observations of Knh by TEM show surface fibers with significant amounts of curvilinearity. Additionally, examining Knh-mediated adherence

using shear resistance adherence assays, we observed a positive relationship between shear stress and level of adherence. This relationship is a classic indicator of an adhesive interaction between a flexible adhesin and its receptor that is enhanced by force, termed catch-bond adherence (Sokurenko, Vogel et al. 2008). These data suggest that Knh is flexible and that this flexibility contributes to Knh-mediated adherence.

AFM and similar methods that measure the force of adherence between two interacting proteins offer an interesting supplement to the typical ELISA used to determine the affinity of a receptor/ligand interaction. AFM probe tips can be functionalized by coating them with purified Knh or by adhering bacteria producing Knh to the AFM tips. A functionalized AFM tip is allowed to adhere to a substrate coated with the desired receptor or host cells and is then pulled away with some constant velocity. The force of the adhesive bond is measured by the displacement of the probe tip, the magnitude of which is proportional to the actual force exerted on the probe tip. A similar experiment can be done using optical tweezers and beads coated with purified Knh and purified Knh receptor.

The advantage to these methods is that they give a physiologically relevant number, namely the force in Newtons that the adhesin/receptor bond can resist. This number can then be directly compared to the forces that a bacterium could potentially encounter in physiological niches including the flow of the blood stream and the mucociliary

clearance in the pharynx. BcaA (BCAM0224) from *Burkholderia cepacia* can resist pulling forces exerted by AFM of 64-85 pN, depending on the speed of the probe retraction (El-Kirat-Chatel, Mil-Homens et al. 2013). Interestingly, the force of adherence and the rupture length of the bond increased with increasing speed of retraction, in agreement with our flow adherence assays. For reference, the shear forces exerted at the mucosal layer by airflow in the respiratory tract is reported to be 0.5 - 2.0 dynes, where 1 dyne is equal to 10 μ N (Green 2004).

An added benefit of using AFM or optical tweezers is that subtle characteristics of the adhesin/receptor bond can be unraveled. For example, in experiments using AFM to pull T4P off a surface (Lu, Giuliani et al. 2015), analysis of the force curves generated revealed that the pilus is capable of adhering along its length. Furthermore, this adherence was localized to several discrete points along the pilus. This is evidenced by multiple peaks in the force curves as each adhesive bond ruptures in turn when individual pili are pulled, for example, by AFM. This information suggests that adherence activity is distributed within the pilus. All studies examining the flexibility of TAAs in relation to their adherence activities have assumed that most or all of the adhesive activity is localized to the most distal region of the passenger domain. However, the growing number of TAAs in which the stalk region also mediates adherence suggests that TAAs may be capable of mediating adherence at multiple points along the passenger domain simultaneously. These characteristics of the adhesin/receptor bond are not apparent by ELISA but are potentially important for the lifestyle of the bacterium. It would be interesting to determine whether the flexibility of

Knh permits it to adhere to host cells and/or ECM proteins at multiple loci along its length simultaneously.

4.4 Define the extent of Knh variation among clinical isolates

One question that we were only able to begin to address is the extent to which Knh varies among clinical isolates. Some attention has been paid to the distribution of the related trimeric autotransporters Hia and Hsf in *H. influenzae* clinical isolates. Hsf is restricted to encapsulated *H. influenzae* strains, while Hia is restricted to nontypable (nonencapsulated) strains. Sequence variation in TAAs has been noted previously with regards to TAA antigenicity (Fusco, Elkins et al. 2013, Malito, Biancucci et al. 2014), but relatively little has been described regarding the effect of sequence variation on TAA activity. This is an area that is a particularly interesting direction of study due to the availability of our large collection of clinical isolates.

We have examined sequences from seven clonal groups, and each PFGE clonal group produces a unique Knh, except PFGE clonal groups J and S, which share a Knh variant. However, there are many more clonal groups/MLST types. To date, there are 73 recognized clonal groups by PFGE and 64 sequence types by DNA uptake sequence typing (Basmaci, Bidet et al. 2014). Because we have such a wide collection of clinical isolates, it would be possible to get a comprehensive understanding of Knh diversity, addressing whether unique Knh domains or sequences are associated with clonal groups. An example of a unique domain is the 193 amino acid insertion in the CSR in

Knh81. These domains and sequences would then be targets for further study to determine their contribution to adhesive activities, antigenicity, and pathogenesis.

4.5 Determine the role of Knh in pathogenesis

It would be interesting to determine the contribution of Knh to *K. kingae* pathogenesis.

There are many roles for Knh that remain to be elucidated: whether Knh mediates adherence *in vivo* to endothelial cells, endocardium, or synovial cells; whether this adherence is necessary for colonization of sites of invasive disease; whether Knh contributes to immune resistance; whether Knh is antigenic; and whether Knh promotes inflammation. Knh could be important in colonization of the posterior pharynx, promoting serum resistance and adaptive immunity evasion, adhering to endothelial and synovial cells, and promoting inflammation.

Concurrent with the work presented here, our lab is in the process of developing several animal models of *K. kingae* infection, including a non-human primate colonization model and an infant rat mortality model. We hope that they will be useful in determining the contribution of various factors to *K. kingae* pathogenesis. In *in vitro* studies we have shown that Knh possesses characteristics suggesting that it is important in colonization and dissemination: It mediates adherence to cells in tissue culture, and this adherence is resistant to shear stress. Knh variants also mediate adherence to ECM proteins, several of which are found in the basal lamina. However, we do not know the role that Knh-mediated adherence plays in colonization or dissemination to sites of invasive

disease. Two relevant *ex vivo* models for bacterial adherence to endothelial cells have been developed and could be exploited to determine the role of Knh in mediating adherence to endothelium and endocardium, in the event an animal model is not forthcoming (Chuang-Smith, Wells et al. 2010, Weidensdorfer, Chae et al. 2015).

Another role that Knh could have in pathogenesis is to promote serum resistance and/or adaptive immunity evasion. It has been shown that binding of complement factors by TAAs, in particular vitronectin, can contribute to serum resistance (Hallstrom, Trajkovska et al. 2006, Leduc, Olsen et al. 2009, Singh, Su et al. 2014). Preliminary work in our lab suggests that Knh does not contribute to serum resistance, despite the evidence that can Knh bind vitronectin. There remain other aspects of innate and adaptive immunity that Knh could be involved in mediating evasion.

4.6 Determine whether Knh is antigenic

It has been demonstrated that TAAs can be activators and targets for the adaptive immune system. As surface proteins, they are prominent potential targets for bactericidal antibodies produced by the adaptive immune system. Malito et al. (2014) used antibody mapping and hydrogen-deuterium exchange mass spectroscopy to determine that bactericidal mAb 33E8 binds the *Neisseria meningitidis* group I TAA NadA3 head region with high affinity, but not to constructs containing only the coiled-coil regions. Furthermore, group I and group II NadA variants are not immunologically cross-reactive despite there being relatively high sequence identity in the epitope bound by

33E8. Group I NadA variants are associated with disease isolates, while group II variants are associated with carrier isolates. A similar phenotype was observed by Fusco et al. (2013) comparing the mAb binding to class I and class II DsrA variants produced by *Haemophilus ducreyi*. Although the mAbs bound both disease and carrier associated variants of class I DsrA variants, the mAbs were not cross reactive with class II variants. These examples suggest that even a modest amount of sequence diversity can significantly change a TAA's antigenicity.

We can generate antibodies to purified fragments of Knh in guinea pigs, but this is not necessarily indicative of the antigenicity of Knh *in vivo* in humans. We have demonstrated that capsule can inhibit Knh-mediated adherence by a steric mechanism. The masking of Knh by capsule also suggests that the capsule can block antibodies from binding to Knh. However, bacteria that have lysed or have been phagocytosed by phagocytes would be a source of antigens available to the adaptive immune system *in vivo*. Therefore Knh is a potential source of epitopes for antibody production.

Additionally, if we consider the amino acid sequence of Knh, it would be reasonable to hypothesize that the variability of the VSR is to avoid detection by the adaptive immune system. A corollary to this hypothesis is that the YLHD and conserved region of the stalk are either poorly antigenic or are functionally important, thus limiting the amount of variation these regions can tolerate. The example of NadA summarized previously suggests that even the small amounts of variation we observed in the YLHD and CSR

has the potential to limit the cross reactivity of antibodies to Knh variants. We have generated antisera to both the YLHD and the conserved region of the stalk; however, these antisera were raised against purified fragments. Convalescent serum may be useful in determining the relative antigenicity of the YLHD, the VSR, and the CSR and determining whether antibodies to Knh can be bactericidal.

4.7 Knh and virulence gene regulation

It has been shown in several cases that TAA expression can regulate the expression of other virulence factors. Qin et al. (2016) observed that the deletion of the TAAs *apa1* and *apa2* in *Actinobacillus pleuropneumoniae* correlated with significant upregulation or downregulation of 72 genes expressed after infection of porcine alveolar macrophages. Interestingly, this included several virulence genes. In the strain deleted for both TAAs, the authors observed upregulation of proteins related to pili and capsule production and downregulation of *tolC*. TolC plays a role in small molecule and toxin secretion (Zgurskaya, Krishnamoorthy et al. 2011) as well as protecting the bacterium from exogenous toxic molecules (Masi and Pages 2013).

Lu et al. (2013) reported that the extreme length and surface density of BadA on the surface of *B. henselae* inhibits the action of the type IV secretion system (T4SS). The *B. henselae* T4SS translocates several effector proteins into the cytoplasm of infected host cells, resulting in uptake of bacterial aggregates via the invasome structure, inhibits apoptosis, and activates a proangiogenic phenotype. Wild type BadA prevented the

translocation of effector proteins, likely by preventing intimate contact with the host cell due to its length. In a study of clinical isolates, it was found that expression of BadA largely correlated negatively with the expression of the T4SS and vice versa, suggesting that BadA and T4SS are differentially expressed during colonization and invasion.

These examples suggest that *knh* expression has the potential to regulate other genes expressed by *K. kingae*. The mechanism of regulation could be genetic, as in the case of *apa1* and *apa2*, or mechanical, as in the case of *badA*. No clinical isolate that we have examined has been shown to lack Knh production (data not shown), suggesting that *knh* is constitutively expressed. However, our prototype strain KK01 has a genetically identical variant KK03 that produces a significantly greater amount of Knh (Kern, Porsch et al. 2017). This observation suggests the possibility that *knh* itself is differentially expressed and KK01 and KK03 may provide insight into genes regulated downstream of *knh*.

One virulence factor that may be particularly interesting in the context of invasion and pathogenesis is the potent RTX toxin produced by *K. kingae*. RTX toxins are a family of pore-forming exotoxins produced by gram-negative bacteria (Benz 2016), and are members the larger superfamily of RTX-like proteins which have a large diversity of functions. RTX toxins can have diverse targets, though several members of the family have been described as being preferentially leukotoxins (Lally, Hill et al. 1999). At low concentrations, RTX toxins induce cell apoptosis, whereas at high concentrations they

are capable of forming pores in the cell membrane. More recently, it has been reported that RTX toxin (HlyA) proteins associated with outer membrane vesicles (OMVs) of *E. coli* cause host cell death by triggering caspase-9-mediated apoptosis, while free secreted RTX toxin proteins form pores in endothelial cells (Bielaszewska, Aldick et al. 2014). In *K. kingae*, the RtxA toxin is a pore forming toxin (Barcena-Uribarri, Benz et al. 2015) that is significantly cytotoxic to host cells *in vitro* (Kehl-Fie and St Geme 2007) and contributes significantly to virulence in an infant rat model (Chang, Nudell et al. 2014). The *Knh* RtxA toxin locus also encodes several auxiliary proteins that are involved in the production and secretion of the toxin (Kehl-Fie and St Geme 2007). *K. kingae* further encodes a *tolC* homologue which is predicted to be involved in RtxA secretion. RtxA is also associated with OMVs produced by *K. kingae* (Maldonado, Wei et al. 2011).

Experiments showing the activity of RtxA have used purified OMVs and RtxA protein. However, in a physiological niche, the actual concentration of RtxA is likely to be significantly lower. Close adherence to host cells would increase the local concentration of RtxA proteins and OMVs at the host cell surface and thus increase the activity of RtxA. It could be hypothesized that nonadherent bacteria primarily cause cell death by RtxA-mediated apoptosis while adherent bacteria have increased RtxA pore formation. In previous work, we demonstrated that the capsule of *K. kingae* can sterically inhibit *Knh*-mediated adherence and *Knh*-mediated tight adherence is T4P dependent (Porsch, Kehl-Fie et al. 2012, Kern, Porsch et al. 2017). Furthermore, T4P production is positively associated with oropharyngeal and bacteremia isolates and negatively associated with osteoarticular and endocarditis isolates (Kehl-Fie, Porsch et al. 2010). It

would be interesting to examine the effect of T4P, Knh, and capsule expression on RtxA activity, bringing insight to the role of RtxA in invasive *K. kingae* disease.

Bibliography

- Amit, U., R. Dagan and P. Yagupsky (2013). "Prevalence of pharyngeal carriage of *Kingella kingae* in young children and risk factors for colonization." *Pediatr Infect Dis J* **32**(2): 191-193.
- Amit, U., S. Flaishmakher, R. Dagan, N. Porat and P. Yagupsky (2014). "Age-Dependent Carriage of *Kingella kingae* in Young Children and Turnover of Colonizing Strains." *J Pediatric Infect Dis Soc* **3**(2): 160-162.
- Amit, U., N. Porat, R. Basmaci, P. Bidet, S. Bonacorsi, R. Dagan and P. Yagupsky (2012). "Genotyping of invasive *Kingella kingae* isolates reveals predominant clones and association with specific clinical syndromes." *Clin Infect Dis* **55**(8): 1074-1079.
- Anderson de la Llana, R., V. Dubois-Ferriere, A. Maggio, A. Cherkaoui, S. Manzano, G. Renzi, J. Hibbs, J. Schrenzel and D. Ceroni (2015). "Oropharyngeal *Kingella kingae* carriage in children: characteristics and correlation with osteoarticular infections." *Pediatr Res* **78**(5): 574-579.
- Aoki, E., D. Sato, K. Fujiwara and M. Ikeguchi (2017). "Electrostatic Repulsion between Unique Arginine Residues Is Essential for the Efficient in Vitro Assembly of the Transmembrane Domain of a Trimeric Autotransporter." *Biochemistry* **56**(15): 2139-2148.
- Babb, J. L. and C. S. Cummins (1978). "Encapsulation of Bacteroides species." *Infect Immun* **19**(3): 1088-1091.
- Bambini, S., M. De Chiara, A. Muzzi, M. Mora, J. Lucidarme, C. Brehony, R. Borrow, V. Massignani, M. Comanducci, M. C. Maiden, R. Rappuoli, M. Pizza and K. A. Jolley (2014). "Neisseria adhesin A variation and revised nomenclature scheme." *Clin Vaccine Immunol* **21**(7): 966-971.
- Barcena-Uribarri, I., R. Benz, M. Winterhalter, E. Zakharian and N. Balashova (2015). "Pore forming activity of the potent RTX-toxin produced by pediatric pathogen *Kingella kingae*: Characterization and comparison to other RTX-family members." *Biochim Biophys Acta* **1848**(7): 1536-1544.
- Basmaci, R., P. Bidet, P. Yagupsky, C. Munoz-Almagro, N. V. Balashova, C. Doit and S. Bonacorsi (2014). "Major intercontinentally distributed sequence types of *Kingella kingae* and development of a rapid molecular typing tool." *J Clin Microbiol* **52**(11): 3890-3897.
- Basmaci, R., S. Bonacorsi, B. Ilharreborde, C. Doit, M. Lorrot, M. Kahil, B. Visseaux, N. Houhou and P. Bidet (2015). "High respiratory virus oropharyngeal carriage rate during *Kingella kingae* osteoarticular infections in children." *Future Microbiol* **10**(1): 9-14.

Basmaci, R., B. Ilharreborde, P. Bidet, C. Doit, M. Lorrot, K. Mazda, E. Bingen and S. Bonacorsi (2012). "Isolation of *Kingella kingae* in the oropharynx during *K. kingae* arthritis in children." Clin Microbiol Infect **18**(5): E134-136.

Beaussart, A., A. E. Baker, S. L. Kuchma, S. El-Kirat-Chatel, G. A. O'Toole and Y. F. Dufrene (2014). "Nanoscale adhesion forces of *Pseudomonas aeruginosa* type IV Pili." ACS Nano **8**(10): 10723-10733.

Benz, R. (2016). "Channel formation by RTX-toxins of pathogenic bacteria: Basis of their biological activity." Biochim Biophys Acta **1858**(3): 526-537.

Berry, J. L. and V. Pelicic (2015). "Exceptionally widespread nanomachines composed of type IV pilins: the prokaryotic Swiss Army knives." FEMS Microbiol Rev **39**(1): 134-154.

Bidet, P., R. Basmaci, J. Guglielmini, C. Doit, C. Jost, A. Birgy and S. Bonacorsi (2016). "Genome Analysis of *Kingella kingae* Strain KWG1 Reveals How a beta-Lactamase Gene Inserted in the Chromosome of This Species." Antimicrob Agents Chemother **60**(1): 703-708.

Bidet, P., E. Collin, R. Basmaci, C. Courroux, V. Prisse, V. Dufour, E. Bingen, E. Grimprel and S. Bonacorsi (2013). "Investigation of an outbreak of osteoarticular infections caused by *Kingella kingae* in a childcare center using molecular techniques." Pediatr Infect Dis J **32**(5): 558-560.

Bielaszewska, M., T. Aldick, A. Bauwens and H. Karch (2014). "Hemolysin of enterohemorrhagic *Escherichia coli*: structure, transport, biological activity and putative role in virulence." Int J Med Microbiol **304**(5-6): 521-529.

Bliska, J. B., M. C. Copass and S. Falkow (1993). "The *Yersinia pseudotuberculosis* adhesin YadA mediates intimate bacterial attachment to and entry into HEp-2 cells." Infect Immun **61**(9): 3914-3921.

Brandle, G., V. Spyropoulou, A. B. Maggio, R. Anderson de la Llana, A. Cherkaoui, G. Renzi, J. Schrenzel, S. Manzano and D. Ceroni (2016). "Identifying Reservoirs of Infections Caused by *Kingella kingae*: A Case-Control Study of Oropharyngeal Carriage of *K. kingae* Among Healthy Adults." Pediatr Infect Dis J **35**(8): 869-871.

Bukholm, G., G. Kapperud and M. Skurnik (1990). "Genetic evidence that the yopA gene-encoded *Yersinia* outer membrane protein Yop1 mediates inhibition of the anti-invasive effect of interferon." Infect Immun **58**(7): 2245-2251.

Ceroni, D., A. Cherkaoui, S. Ferey, A. Kaelin and J. Schrenzel (2010). "*Kingella kingae* osteoarticular infections in young children: clinical features and contribution of a new specific real-time PCR assay to the diagnosis." J Pediatr Orthop **30**(3): 301-304.

Chang, C. Y. (2017). "Surface Sensing for Biofilm Formation in *Pseudomonas aeruginosa*." Front Microbiol **8**: 2671.

- Chang, D. W., Y. A. Nudell, J. Lau, E. Zakharian and N. V. Balashova (2014). "RTX toxin plays a key role in *Kingella kingae* virulence in an infant rat model." Infect Immun **82**(6): 2318-2328.
- China, B., M. P. Sory, B. T. N'Guyen, M. De Bruyere and G. R. Cornelis (1993). "Role of the YadA protein in prevention of opsonization of *Yersinia enterocolitica* by C3b molecules." Infect Immun **61**(8): 3129-3136.
- Chometon, S., Y. Benito, M. Chaker, S. Boisset, C. Ploton, J. Berard, F. Vandenesch and A. M. Freydiere (2007). "Specific real-time polymerase chain reaction places *Kingella kingae* as the most common cause of osteoarticular infections in young children." Pediatr Infect Dis J **26**(5): 377-381.
- Chuang-Smith, O. N., C. L. Wells, M. J. Henry-Stanley and G. M. Dunny (2010). "Acceleration of *Enterococcus faecalis* biofilm formation by aggregation substance expression in an *ex vivo* model of cardiac valve colonization." PLoS One **5**(12): e15798.
- Clausen, M., V. Jakovljevic, L. Sogaard-Andersen and B. Maier (2009). "High-force generation is a conserved property of type IV pilus systems." J Bacteriol **191**(14): 4633-4638.
- Comanducci, M., S. Bambini, D. A. Caugant, M. Mora, B. Brunelli, B. Capecchi, L. Ciocchi, R. Rappuoli and M. Pizza (2004). "NadA diversity and carriage in *Neisseria meningitidis*." Infect Immun **72**(7): 4217-4223.
- Cook, G. S., J. W. Costerton and R. J. Lamont (1998). "Biofilm formation by *Porphyromonas gingivalis* and *Streptococcus gordonii*." J Periodontal Res **33**(6): 323-327.
- Cotter, S. E., N. K. Surana and J. W. St Geme, 3rd (2005). "Trimeric autotransporters: a distinct subfamily of autotransporter proteins." Trends Microbiol **13**(5): 199-205.
- Dahlback, B. and E. R. Podack (1985). "Characterization of human S protein, an inhibitor of the membrane attack complex of complement. Demonstration of a free reactive thiol group." Biochemistry **24**(9): 2368-2374.
- Dautin, N. and H. D. Bernstein (2007). "Protein secretion in gram-negative bacteria via the autotransporter pathway." Annu Rev Microbiol **61**: 89-112.
- Droz, N., V. Enouf, P. Bidet, D. Mohamed, S. Behillil, A. L. Simon, M. Bachy, M. Caseris, S. Bonacorsi and R. Basmaci (2018). "Temporal Association Between Rhinovirus Activity and *Kingella kingae* Osteoarticular Infections." J Pediatr **192**: 234-239 e232.
- Duddridge, J. E., C. A. Kent and J. F. Laws (1982). "Effect of surface shear stress on the attachment of *Pseudomonas fluorescens* to stainless steel under defined flow conditions." Biotechnol Bioeng **24**(1): 153-164.

- El-Kirat-Chatel, S., D. Mil-Homens, A. Beaussart, A. M. Fialho and Y. F. Dufrene (2013). "Single-molecule atomic force microscopy unravels the binding mechanism of a *Burkholderia cenocepacia* trimeric autotransporter adhesin." Mol Microbiol **89**(4): 649-659.
- El Houmami, N., J. Bzdrenga, G. A. Durand, P. Minodier, H. Seligmann, E. Prudent, S. Bakour, S. Bonacorsi, D. Raoult, P. Yagupsky and P. E. Fournier (2017). "Molecular Tests That Target the RTX Locus Do Not Distinguish between *Kingella kingae* and the Recently Described *Kingella negevensis* Species." J Clin Microbiol **55**(10): 3113-3122.
- El Houmami, N., P. E. Fournier and D. Ceroni (2017). "Targeting the *Kingella Kingae* groEL Gene is a Reliable Method for the Molecular Diagnosis of *K. Kingae* Infection and Carriage." J Paediatr Child Health **53**(10): 1030-1031.
- Felsenstein, J. (1985). "Confidence Limits on Phylogenies: An Approach Using the Bootstrap." Evolution **39**(4): 783-791.
- Fusco, W. G., C. Elkins and I. Leduc (2013). "Trimeric autotransporter DsrA is a major mediator of fibrinogen binding in *Haemophilus ducreyi*." Infect Immun **81**(12): 4443-4452.
- Gene, A., J. J. Garcia-Garcia, P. Sala, M. Sierra and R. Huguet (2004). "Enhanced culture detection of *Kingella kingae*, a pathogen of increasing clinical importance in pediatrics." Pediatr Infect Dis J **23**(9): 886-888.
- Gravel, J., D. Ceroni, L. Lacroix, C. Renaud, G. Grimard, E. Samara, A. Cherkaoui, G. Renzi, J. Schrenzel and S. Manzano (2017). "Association between oropharyngeal carriage of *Kingella kingae* and osteoarticular infection in young children: a case-control study." CMAJ **189**(35): E1107-E1111.
- Green, A. S. (2004). "Modelling of peak-flow wall shear stress in major airways of the lung." J Biomech **37**(5): 661-667.
- Grin, I., M. D. Hartmann, G. Sauer, B. Hernandez Alvarez, M. Schutz, S. Wagner, J. Madlung, B. Macek, A. Felipe-Lopez, M. Hensel, A. Lupas and D. Linke (2014). "A trimeric lipoprotein assists in trimeric autotransporter biogenesis in enterobacteria." J Biol Chem **289**(11): 7388-7398.
- Hallstrom, T. and K. Riesbeck (2010). "*Haemophilus influenzae* and the complement system." Trends Microbiol **18**(6): 258-265.
- Hallstrom, T., E. Trajkovska, A. Forsgren and K. Riesbeck (2006). "*Haemophilus influenzae* surface fibrils contribute to serum resistance by interacting with vitronectin." J Immunol **177**(1): 430-436.
- Henriksen, S. D. and K. Bovre (1968). "*Moraxella kingii* sp.nov., a haemolytic, saccharolytic species of the genus *Moraxella*." J Gen Microbiol **51**(3): 377-385.

Henriksen, S. D. K. B. (1976). "Transfer of *Moraxella-kingae* *Kingella*-Henriksen and Bovre to Genus Gen-Nov in Family Neisseriaceae." Int J Syst Bacteriol **26**: 447-450.

Hill, D. J., N. J. Griffiths, E. Borodina and M. Virji (2010). "Cellular and molecular biology of *Neisseria meningitidis* colonization and invasive disease." Clin Sci (Lond) **118**(9): 547-564.

Hoiczky, E., A. Roggenkamp, M. Reichenbecher, A. Lupas and J. Heesemann (2000). "Structure and sequence analysis of *Yersinia* YadA and *Moraxella* UspAs reveal a novel class of adhesins." Embo j **19**(22): 5989-5999.

Horton, M. A. (1997). "The alpha v beta 3 integrin "vitronectin receptor"." Int J Biochem Cell Biol **29**(5): 721-725.

Hospenthal, M. K., T. R. D. Costa and G. Waksman (2017). "A comprehensive guide to pilus biogenesis in Gram-negative bacteria." Nat Rev Microbiol **15**(6): 365-379.

Ishikawa, M., S. Yoshimoto, A. Hayashi, J. Kanie and K. Hori (2016). "Discovery of a novel periplasmic protein that forms a complex with a trimeric autotransporter adhesin and peptidoglycan." Mol Microbiol **101**(3): 394-410.

Jin, F., J. C. Conrad, M. L. Gibiansky and G. C. Wong (2011). "Bacteria use type-IV pili to slingshot on surfaces." Proc Natl Acad Sci U S A **108**(31): 12617-12622.

Kaiser, P. O., D. Linke, H. Schwarz, J. C. Leo and V. A. Kempf (2012). "Analysis of the BadA stalk from *Bartonella henselae* reveals domain-specific and domain-overlapping functions in the host cell infection process." Cell Microbiol **14**(2): 198-209.

Katoh, K., J. Rozewicki and K. D. Yamada (2017). "MAFFT online service: multiple sequence alignment, interactive sequence choice and visualization." Brief Bioinform.

Kehl-Fie, T. E., S. E. Miller and J. W. St Geme, 3rd (2008). "*Kingella kingae* expresses type IV pili that mediate adherence to respiratory epithelial and synovial cells." J Bacteriol **190**(21): 7157-7163.

Kehl-Fie, T. E., E. A. Porsch, S. E. Miller and J. W. St Geme, 3rd (2009). "Expression of *Kingella kingae* type IV pili is regulated by sigma54, PilS, and PilR." J Bacteriol **191**(15): 4976-4986.

Kehl-Fie, T. E., E. A. Porsch, P. Yagupsky, E. A. Grass, C. Obert, D. K. Benjamin, Jr. and J. W. St Geme, 3rd (2010). "Examination of type IV pilus expression and pilus-associated phenotypes in *Kingella kingae* clinical isolates." Infect Immun **78**(4): 1692-1699.

Kehl-Fie, T. E. and J. W. St Geme, 3rd (2007). "Identification and characterization of an RTX toxin in the emerging pathogen *Kingella kingae*." J Bacteriol **189**(2): 430-436.

- Kern, B. K., E. A. Porsch and J. W. St Geme, 3rd (2017). "Defining the Mechanical Determinants of *Kingella kingae* Adherence to Host Cells." J Bacteriol **199**(23).
- Khatami, A., B. R. Rivers, A. C. Outhred and A. M. Kesson (2017). "Low prevalence of *Kingella kingae* carriage in children aged 6-48 months in Sydney, Australia." J Paediatr Child Health **53**(2): 170-172.
- Kiang, K. M., F. Ogunmodede, B. A. Juni, D. J. Boxrud, A. Glennen, J. M. Bartkus, E. A. Cebelinski, K. Harriman, S. Koop, R. Faville, R. Danila and R. Lynfield (2005). "Outbreak of osteomyelitis/septic arthritis caused by *Kingella kingae* among child care center attendees." Pediatrics **116**(2): e206-213.
- Koiwai, K., M. D. Hartmann, D. Linke, A. N. Lupas and K. Hori (2016). "Structural Basis for Toughness and Flexibility in the C-terminal Passenger Domain of an *Acinetobacter* Trimeric Autotransporter Adhesin." J Biol Chem **291**(8): 3705-3724.
- Laarmann, S., D. Cutter, T. Juehne, S. J. Barenkamp and J. W. St Geme (2002). "The *Haemophilus influenzae* Hia autotransporter harbours two adhesive pockets that reside in the passenger domain and recognize the same host cell receptor." Mol Microbiol **46**(3): 731-743.
- Lally, E. T., R. B. Hill, I. R. Kieba and J. Korostoff (1999). "The interaction between RTX toxins and target cells." Trends Microbiol **7**(9): 356-361.
- Lanave, C., G. Preparata, C. Saccone and G. Serio (1984). "A new method for calculating evolutionary substitution rates." J Mol Evol **20**(1): 86-93.
- Lazar Adler, N. R., R. E. Dean, R. J. Saint, M. P. Stevens, J. L. Prior, T. P. Atkins and E. E. Galyov (2013). "Identification of a predicted trimeric autotransporter adhesin required for biofilm formation of *Burkholderia pseudomallei*." PLoS One **8**(11): e79461.
- Leduc, I., B. Olsen and C. Elkins (2009). "Localization of the domains of the *Haemophilus ducreyi* trimeric autotransporter DsrA involved in serum resistance and binding to the extracellular matrix proteins fibronectin and vitronectin." Infect Immun **77**(2): 657-666.
- Lehours, P., A. M. Freydiere, O. Richer, C. Burucoa, S. Boisset, P. Lanotte, M. F. Prere, A. Ferroni, C. Lafuente, F. Vandenesch, F. Megraud and A. Menard (2011). "The rtxA toxin gene of *Kingella kingae*: a pertinent target for molecular diagnosis of osteoarticular infections." J Clin Microbiol **49**(4): 1245-1250.
- Lehr, U., M. Schutz, P. Oberhettinger, F. Ruiz-Perez, J. W. Donald, T. Palmer, D. Linke, I. R. Henderson and I. B. Autenrieth (2010). "C-terminal amino acid residues of the trimeric autotransporter adhesin YadA of *Yersinia enterocolitica* are decisive for its recognition and assembly by BamA." Mol Microbiol **78**(4): 932-946.

Leighton, T. L., R. N. Buensuceso, P. L. Howell and L. L. Burrows (2015). "Biogenesis of *Pseudomonas aeruginosa* type IV pili and regulation of their function." Environ Microbiol **17**(11): 4148-4163.

Leong, C. G., R. A. Bloomfield, C. A. Boyd, A. J. Dornbusch, L. Lieber, F. Liu, A. Owen, E. Slay, K. M. Lang and C. P. Lostroh (2017). "The role of core and accessory type IV pilus genes in natural transformation and twitching motility in the bacterium *Acinetobacter baylyi*." PLoS One **12**(8): e0182139.

Lu, S., M. Giuliani, H. Harvey, L. L. Burrows, R. A. Wickham and J. R. Dutcher (2015). "Nanoscale Pulling of Type IV Pili Reveals Their Flexibility and Adhesion to Surfaces over Extended Lengths of the Pili." Biophys J **108**(12): 2865-2875.

Lu, Y. Y., B. Franz, M. C. Truttmann, T. Riess, J. Gay-Fraret, M. Faustmann, V. A. Kempf and C. Dehio (2013). "*Bartonella henselae* trimeric autotransporter adhesin BadA expression interferes with effector translocation by the VirB/D4 type IV secretion system." Cell Microbiol **15**(5): 759-778.

Lyskowski, A., J. C. Leo and A. Goldman (2011). "Structure and biology of trimeric autotransporter adhesins." Adv Exp Med Biol **715**: 143-158.

Maier, B., L. Potter, M. So, C. D. Long, H. S. Seifert and M. P. Sheetz (2002). "Single pilus motor forces exceed 100 pN." Proc Natl Acad Sci U S A **99**(25): 16012-16017.

Maier, B. and G. C. L. Wong (2015). "How Bacteria Use Type IV Pili Machinery on Surfaces." Trends Microbiol **23**(12): 775-788.

Maldonado, R., R. Wei, S. C. Kachlany, M. Kazi and N. V. Balashova (2011). "Cytotoxic effects of *Kingella kingae* outer membrane vesicles on human cells." Microb Pathog **51**(1-2): 22-30.

Malito, E., M. Biancucci, A. Faleri, I. Ferlenghi, M. Scarselli, G. Maruggi, P. Lo Surdo, D. Veggi, A. Liguori, L. Santini, I. Bertoldi, R. Petracca, S. Marchi, G. Romagnoli, E. Cartocci, I. Vercellino, S. Savino, G. Spraggon, N. Norais, M. Pizza, R. Rappuoli, V. Maignani and M. J. Bottomley (2014). "Structure of the meningococcal vaccine antigen NadA and epitope mapping of a bactericidal antibody." Proc Natl Acad Sci U S A **111**(48): 17128-17133.

Masi, M. and J. M. Pages (2013). "Structure, Function and Regulation of Outer Membrane Proteins Involved in Drug Transport in Enterobacteriaceae: the OmpF/C - TolC Case." Open Microbiol J **7**: 22-33.

Merz, A. J., M. So and M. P. Sheetz (2000). "Pilus retraction powers bacterial twitching motility." Nature **407**(6800): 98-102.

Miajlovic, H. and S. G. Smith (2014). "Bacterial self-defence: how *Escherichia coli* evades serum killing." FEMS Microbiol Lett **354**(1): 1-9.

- Mikula, K. M., J. C. Leo, A. Lyskowski, S. Kedracka-Krok, A. Pirog and A. Goldman (2012). "The translocation domain in trimeric autotransporter adhesins is necessary and sufficient for trimerization and autotransportation." J Bacteriol **194**(4): 827-838.
- Mil-Homens, D., S. N. Pinto, R. G. Matos, C. Arraiano and A. M. Fialho (2017). "*Burkholderia cenocepacia* K56-2 trimeric autotransporter adhesin BcaA binds TNFR1 and contributes to induce airway inflammation." Cell Microbiol **19**(4).
- Misawa, Y., K. A. Kelley, X. Wang, L. Wang, W. B. Park, J. Birtel, D. Saslowsky and J. C. Lee (2015). "*Staphylococcus aureus* Colonization of the Mouse Gastrointestinal Tract Is Modulated by Wall Teichoic Acid, Capsule, and Surface Proteins." PLoS Pathog **11**(7): e1005061.
- Mularski, A., J. J. Wilksch, E. Hanssen, R. A. Strugnell and F. Separovic (2016). "Atomic force microscopy of bacteria reveals the mechanobiology of pore forming peptide action." Biochim Biophys Acta **1858**(6): 1091-1098.
- Nagel, J. A., R. B. Dickinson and S. L. Cooper (1996). "Bacterial adhesion to polyurethane surfaces in the presence of pre-adsorbed high molecular weight kininogen." J Biomater Sci Polym Ed **7**(9): 769-780.
- Nejadnik, M. R., H. C. van der Mei, H. J. Busscher and W. Norde (2008). "Determination of the shear force at the balance between bacterial attachment and detachment in weak-adherence systems, using a flow displacement chamber." Appl Environ Microbiol **74**(3): 916-919.
- Niddam, A. F., R. Ebady, A. Bansal, A. Koehler, B. Hinz and T. J. Moriarty (2017). "Plasma fibronectin stabilizes *Borrelia burgdorferi*-endothelial interactions under vascular shear stress by a catch-bond mechanism." Proc Natl Acad Sci U S A **114**(17): E3490-E3498.
- Oder, M., R. Fink, K. Bohinc and K. G. Torkar (2017). "The influence of shear stress on the adhesion capacity of *Legionella pneumophila*." Arh Hig Rada Toksikol **68**(2): 109-115.
- Olijve, L., R. Podmore, T. Anderson and T. Walls (2016). "High rate of oropharyngeal *Kingella kingae* carriage in New Zealand children." J Paediatr Child Health **52**(12): 1081-1085.
- Oomen, C. J., P. van Ulsen, P. van Gelder, M. Feijen, J. Tommassen and P. Gros (2004). "Structure of the translocator domain of a bacterial autotransporter." EMBO J **23**(6): 1257-1266.
- Pattengale, N. D., M. Alipour, O. R. Bininda-Emonds, B. M. Moret and A. Stamatakis (2010). "How many bootstrap replicates are necessary?" J Comput Biol **17**(3): 337-354.
- Pilz, D., T. Vocke, J. Heesemann and V. Brade (1992). "Mechanism of YadA-mediated serum resistance of *Yersinia enterocolitica* serotype O3." Infect Immun **60**(1): 189-195.

Pina, S., A. Olvera, A. Barcelo and A. Bensaid (2009). "Trimeric autotransporters of *Haemophilus parasuis*: generation of an extensive passenger domain repertoire specific for pathogenic strains." J Bacteriol **191**(2): 576-587.

Porsch, E. A., T. E. Kehl-Fie and J. W. St Geme, 3rd (2012). "Modulation of *Kingella kingae* adherence to human epithelial cells by type IV Pili, capsule, and a novel trimeric autotransporter." MBio **3**(5).

Porsch, E. A., K. F. Starr, P. Yagupsky and J. W. St Geme, 3rd (2017). "The Type a and Type b Polysaccharide Capsules Predominate in an International Collection of Invasive *Kingella kingae* Isolates." mSphere **2**(2).

Qin, W., L. Wang, R. Zhai, Q. Ma, J. Liu, C. Bao, H. Zhang, C. Sun, X. Feng, J. Gu, C. Du, W. Han, P. R. Langford and L. Lei (2016). "Trimeric autotransporter adhesins contribute to *Actinobacillus pleuropneumoniae* pathogenicity in mice and regulate bacterial gene expression during interactions between bacteria and porcine primary alveolar macrophages." Antonie Van Leeuwenhoek **109**(1): 51-70.

Qu, J., C. Mayer, S. Behrens, O. Holst and J. H. Kleinschmidt (2007). "The trimeric periplasmic chaperone Skp of *Escherichia coli* forms 1:1 complexes with outer membrane proteins via hydrophobic and electrostatic interactions." J Mol Biol **374**(1): 91-105.

Reimann, K., H. Heise and J. Blom (1988). "Attempts to demonstrate a polysaccharide capsule in *Neisseria gonorrhoeae*." APMIS **96**(8): 735-740.

Rempe, K. A., L. A. Spruce, E. A. Porsch, S. H. Seeholzer, N. Norskov-Lauritsen and J. W. St Geme, 3rd (2015). "Unconventional N-Linked Glycosylation Promotes Trimeric Autotransporter Function in *Kingella kingae* and *Aggregatibacter aphrophilus*." MBio **6**(4).

Richardson, W. P. and J. C. Sadoff (1977). "Production of a capsule of *Neisseria gonorrhoeae*." Infect Immun **15**(2): 663-664.

Sena, A. C., P. Seed, B. Nicholson, M. Joyce and C. K. Cunningham (2010). "*Kingella kingae* endocarditis and a cluster investigation among daycare attendees." Pediatr Infect Dis J **29**(1): 86-88.

Sievers, F., A. Wilm, D. Dineen, T. J. Gibson, K. Karplus, W. Li, R. Lopez, H. McWilliam, M. Remmert, J. Soding, J. D. Thompson and D. G. Higgins (2011). "Fast, scalable generation of high-quality protein multiple sequence alignments using Clustal Omega." Mol Syst Biol **7**: 539.

Singh, B., Y. C. Su, T. Al-Jubair, O. Mukherjee, T. Hallstrom, M. Morgelin, A. M. Blom and K. Riesbeck (2014). "A fine-tuned interaction between trimeric autotransporter haemophilus surface fibrils and vitronectin leads to serum resistance and adherence to respiratory epithelial cells." Infect Immun **82**(6): 2378-2389.

- Skerker, J. M. and H. C. Berg (2001). "Direct observation of extension and retraction of type IV pili." Proc Natl Acad Sci U S A **98**(12): 6901-6904.
- Skurnik, M., Y. el Tahir, M. Saarinen, S. Jalkanen and P. Toivanen (1994). "YadA mediates specific binding of enteropathogenic *Yersinia enterocolitica* to human intestinal submucosa." Infect Immun **62**(4): 1252-1261.
- Slonim, A., M. Steiner and P. Yagupsky (2003). "Immune response to invasive *Kingella kingae* infections, age-related incidence of disease, and levels of antibody to outer-membrane proteins." Clin Infect Dis **37**(4): 521-527.
- Slonim, A., E. S. Walker, E. Mishori, N. Porat, R. Dagan and P. Yagupsky (1998). "Person-to-person transmission of *Kingella kingae* among day care center attendees." J Infect Dis **178**(6): 1843-1846.
- Sokurenko, E. V., V. Vogel and W. E. Thomas (2008). "Catch-bond mechanism of force-enhanced adhesion: counterintuitive, elusive, but ... widespread?" Cell Host Microbe **4**(4): 314-323.
- Spyropoulou, V., G. Brandle, A. B. R. Maggio, R. Anderson Della Llana, A. Cherkaoui, G. Renzi, J. Schrenzel, S. Manzano and D. Ceroni (2017). "A transversal pilot study of oropharyngeal carriage of *Kingella kingae* in healthy children younger than 6 months." World J Pediatr **13**(6): 615-617.
- Stamatakis, A. (2006). "RAxML-VI-HPC: maximum likelihood-based phylogenetic analyses with thousands of taxa and mixed models." Bioinformatics **22**(21): 2688-2690.
- Starr, K. F., E. A. Porsch, P. C. Seed, C. Heiss, R. Naran, L. S. Forsberg, U. Amit, P. Yagupsky, P. Azadi and J. W. St Geme, 3rd (2016). "*Kingella kingae* Expresses Four Structurally Distinct Polysaccharide Capsules That Differ in Their Correlation with Invasive Disease." PLoS Pathog **12**(10): e1005944.
- Starr, K. F., E. A. Porsch, P. C. Seed and J. W. St Geme, 3rd (2016). "Genetic and Molecular Basis of *Kingella kingae* Encapsulation." Infect Immun **84**(6): 1775-1784.
- Strom, M. S., D. N. Nunn and S. Lory (1994). "Posttranslational processing of type IV prepilin and homologs by PilD of *Pseudomonas aeruginosa*." Methods Enzymol **235**: 527-540.
- Strouts, F. R., P. Power, N. J. Croucher, N. Corton, A. van Tonder, M. A. Quail, P. R. Langford, M. J. Hudson, J. Parkhill, J. S. Kroll and S. D. Bentley (2012). "Lineage-specific virulence determinants of *Haemophilus influenzae* biogroup aegyptius." Emerg Infect Dis **18**(3): 449-457.
- Stukalov, O., A. Korenevsky, T. J. Beveridge and J. R. Dutcher (2008). "Use of atomic force microscopy and transmission electron microscopy for correlative studies of bacterial capsules." Appl Environ Microbiol **74**(17): 5457-5465.

- Surana, N. K., D. Cutter, S. J. Barenkamp and J. W. St Geme, 3rd (2004). "The Haemophilus influenzae Hia autotransporter contains an unusually short trimeric translocator domain." J Biol Chem **279**(15): 14679-14685.
- Szczesny, P., D. Linke, A. Ursinus, K. Bar, H. Schwarz, T. M. Riess, V. A. Kempf, A. N. Lupas, J. Martin and K. Zeth (2008). "Structure of the head of the *Bartonella adhesin* BadA." PLoS Pathog **4**(8): e1000119.
- Szczesny, P. and A. Lupas (2008). "Domain annotation of trimeric autotransporter adhesins--daTAA." Bioinformatics **24**(10): 1251-1256.
- Szlavik, J., D. S. Paiva, N. Mork, F. van den Berg, J. Verran, K. Whitehead, S. Knochel and D. S. Nielsen (2012). "Initial adhesion of *Listeria monocytogenes* to solid surfaces under liquid flow." Int J Food Microbiol **152**(3): 181-188.
- Tamm, A., A. M. Tarkkanen, T. K. Korhonen, P. Kuusela, P. Toivanen and M. Skurnik (1993). "Hydrophobic domains affect the collagen-binding specificity and surface polymerization as well as the virulence potential of the YadA protein of *Yersinia enterocolitica*." Mol Microbiol **10**(5): 995-1011.
- Terti, R., M. Skurnik, T. Vartio and P. Kuusela (1992). "Adhesion protein YadA of *Yersinia* species mediates binding of bacteria to fibronectin." Infect Immun **60**(7): 3021-3024.
- Thomas, W. E., L. M. Nilsson, M. Forero, E. V. Sokurenko and V. Vogel (2004). "Shear-dependent 'stick-and-roll' adhesion of type 1 fimbriated *Escherichia coli*." Mol Microbiol **53**(5): 1545-1557.
- Thomas, W. E., E. Trintchina, M. Forero, V. Vogel and E. V. Sokurenko (2002). "Bacterial adhesion to target cells enhanced by shear force." Cell **109**(7): 913-923.
- Thomen, P., J. Robert, A. Monmeyran, A. F. Bitbol, C. Douarche and N. Henry (2017). "Bacterial biofilm under flow: First a physical struggle to stay, then a matter of breathing." PLoS One **12**(4): e0175197.
- Tu, T. Y., M. K. Hsieh, D. H. Tan, S. C. Ou, J. H. Shien, T. Y. Yen and P. C. Chang (2015). "Loss of the Capsule Increases the Adherence Activity but Decreases the Virulence of *Avibacterium paragallinarum*." Avian Dis **59**(1): 87-93.
- Veloso, T. R., J. Claes, S. Van Kerckhoven, B. Ditkowski, L. G. Hurtado-Aguilar, S. Jockenhoevel, P. Mela, R. Jashari, M. Gewillig, M. F. Hoylaerts, B. Meyns and R. Heying (2018). "Bacterial adherence to graft tissues in static and flow conditions." J Thorac Cardiovasc Surg **155**(1): 325-332 e324.
- Verdier, I., A. Gayet-Ageron, C. Ploton, P. Taylor, Y. Benito, A. M. Freydiere, F. Chotel, J. Berard, P. Vanhems and F. Vandenesch (2005). "Contribution of a broad range polymerase chain

reaction to the diagnosis of osteoarticular infections caused by *Kingella kingae*: description of twenty-four recent pediatric diagnoses." Pediatr Infect Dis J **24**(8): 692-696.

Viljanen, J., K. Lounatmaa and P. H. Makela (1991). "Expression of the virulence plasmid-determined protein YOP1 and HeLa cell invasiveness of *Yersinia enterocolitica* O:3." Contrib Microbiol Immunol **12**: 176-181.

Visser, L. G., P. S. Hiemstra, M. T. van den Barselaar, P. A. Ballieux and R. van Furth (1996). "Role of YadA in resistance to killing of *Yersinia enterocolitica* by antimicrobial polypeptides of human granulocytes." Infect Immun **64**(5): 1653-1658.

Voulhoux, R., M. P. Bos, J. Geurtsen, M. Mols and J. Tommassen (2003). "Role of a highly conserved bacterial protein in outer membrane protein assembly." Science **299**(5604): 262-265.

Wang, H., J. J. Wilksch, R. A. Strugnell and M. L. Gee (2015). "Role of Capsular Polysaccharides in Biofilm Formation: An AFM Nanomechanics Study." ACS Appl Mater Interfaces **7**(23): 13007-13013.

Wang, L., W. Qin, S. Yang, R. Zhai, L. Zhou, C. Sun, F. Pan, Q. Ji, Y. Wang, J. Gu, X. Feng, C. Du, W. Han, P. R. Langford and L. Lei (2015). "The Adh adhesin domain is required for trimeric autotransporter Apa1-mediated *Actinobacillus pleuropneumoniae* adhesion, autoaggregation, biofilm formation and pathogenicity." Vet Microbiol **177**(1-2): 175-183.

Wang, Y. P., M. K. Hsieh, D. H. Tan, J. H. Shien, S. C. Ou, C. F. Chen and P. C. Chang (2014). "The haemagglutinin of *Avibacterium paragallinarum* is a trimeric autotransporter adhesin that confers haemagglutination, cell adherence and biofilm formation activities." Vet Microbiol **174**(3-4): 474-482.

Weidensdorfer, M., J. I. Chae, C. Makobe, J. Stahl, B. Averhoff, V. Muller, C. Schurmann, R. P. Brandes, G. Wilharm, W. Ballhorn, S. Christ, D. Linke, D. Fischer, S. Gottig and V. A. Kempf (2015). "Analysis of Endothelial Adherence of *Bartonella henselae* and *Acinetobacter baumannii* Using a Dynamic Human Ex Vivo Infection Model." Infect Immun **84**(3): 711-722.

Whitfield, C. (2006). "Biosynthesis and assembly of capsular polysaccharides in *Escherichia coli*." Annu Rev Biochem **75**: 39-68.

Wright, J., M. Thomsen, R. Kolodziejczyk, J. Ridley, J. Sinclair, G. Carrington, B. Singh, K. Riesbeck and A. Goldman (2017). "The crystal structure of PD1, a *Haemophilus* surface fibril domain." Acta Crystallogr F Struct Biol Commun **73**(Pt 2): 101-108.

Yagupsky, P. (2004). "*Kingella kingae*: from medical rarity to an emerging paediatric pathogen." Lancet Infect Dis **4**(6): 358-367.

Yagupsky, P. (2014). "Outbreaks of *Kingella kingae* infections in daycare facilities." Emerg Infect Dis **20**(5): 746-753.

- Yagupsky, P., Y. Ben-Ami, R. Trefler and N. Porat (2016). "Outbreaks of Invasive *Kingella kingae* Infections in Closed Communities." J Pediatr **169**: 135-139 e131.
- Yagupsky, P. and R. Dagan (1997). "*Kingella kingae*: an emerging cause of invasive infections in young children." Clin Infect Dis **24**(5): 860-866.
- Yagupsky, P., R. Dagan, C. W. Howard, M. Einhorn, I. Kassis and A. Simu (1992). "High prevalence of *Kingella kingae* in joint fluid from children with septic arthritis revealed by the BACTEC blood culture system." J Clin Microbiol **30**(5): 1278-1281.
- Yagupsky, P., R. Dagan, F. Prajgrod and M. Merires (1995). "Respiratory carriage of *Kingella kingae* among healthy children." Pediatr Infect Dis J **14**(8): 673-678.
- Yagupsky, P., N. El Houmami and P. E. Fournier (2017). "Outbreaks of Invasive *Kingella kingae* Infections in Daycare Facilities: Approach to Investigation and Management." J Pediatr **182**: 14-20.
- Yagupsky, P., Y. Erlich, S. Ariela, R. Trefler and N. Porat (2006). "Outbreak of *Kingella kingae* skeletal system infections in children in daycare." Pediatr Infect Dis J **25**(6): 526-532.
- Yagupsky, P., N. Peled and O. Katz (2002). "Epidemiological features of invasive *Kingella kingae* infections and respiratory carriage of the organism." J Clin Microbiol **40**(11): 4180-4184.
- Yagupsky, P., N. Porat and E. Pinco (2009). "Pharyngeal colonization by *Kingella kingae* in children with invasive disease." Pediatr Infect Dis J **28**(2): 155-157.
- Yang, Y. and R. R. Isberg (1993). "Cellular internalization in the absence of invasin expression is promoted by the *Yersinia pseudotuberculosis* yadA product." Infect Immun **61**(9): 3907-3913.
- Yang, Z. (1994). "Maximum likelihood phylogenetic estimation from DNA sequences with variable rates over sites: approximate methods." J Mol Evol **39**(3): 306-314.
- Yeo, H. J., S. E. Cotter, S. Laarmann, T. Juehne, J. W. St Geme, 3rd and G. Waksman (2004). "Structural basis for host recognition by the Haemophilus influenzae Hia autotransporter." EMBO J **23**(6): 1245-1256.
- Zgurskaya, H. I., G. Krishnamoorthy, A. Ntrel and S. Lu (2011). "Mechanism and Function of the Outer Membrane Channel TolC in Multidrug Resistance and Physiology of Enterobacteria." Front Microbiol **2**: 189.